

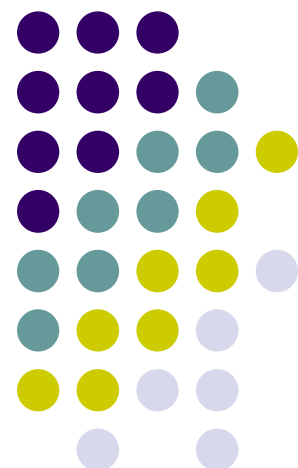
5G基頻傳收機實作

Implementation for the 5G Baseband Transceiver

上課教材



劉宗憲
中正大學通訊工程學系



Outline



- Part I : Fundamentals for the Baseband Transceiver
- Part II : CORDIC Rotation and Its Application
 - Fundamentals of CORDIC Rotation
 - QR-Decomposition of Matrices
 - QR-Decomposition of Matrices for STBC MIMO System
- Part III : Precoding Techniques
 - Precoding Fundamentals
 - Compressed Beamforming Weight Precoding
 - Codebook Based Precoding
- Part IV : Angle of Arrival Estimation
 - Methods for Angle of Arrival Estimation
 - Antenna Calibration





Part I :

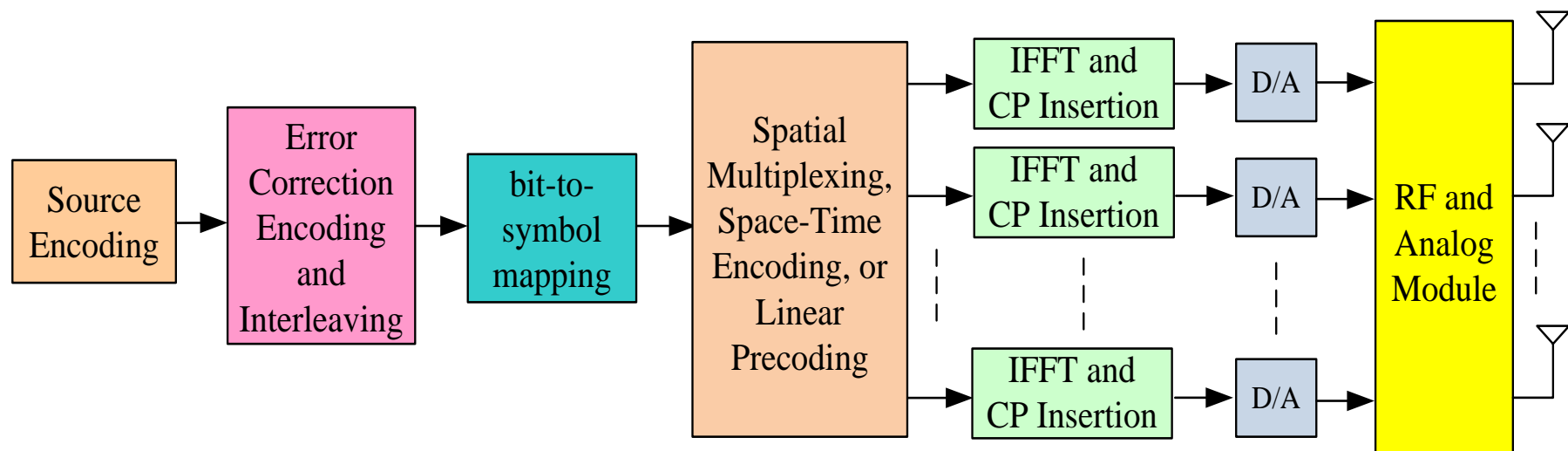
Fundamentals for the Baseband Transceiver





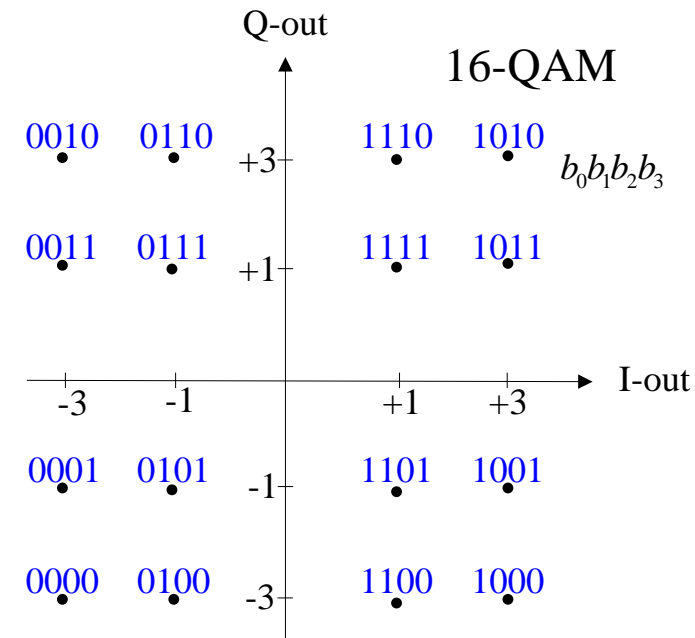
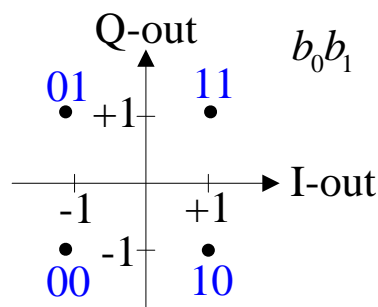
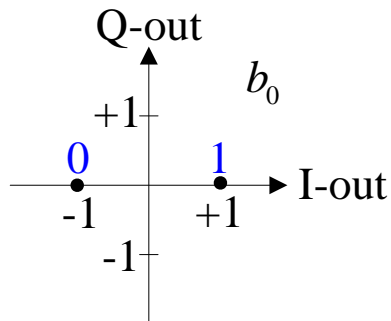
MIMO-OFDM Transmitter

Baseband and Radio Frequency Band Transmitter





Bit to Symbol Mapping





The MIMO Techniques (1/4)

- ◆ The symbol stream is converted in parallel to multiple streams (layers) and then to multiple antennas for transmission.

N_s : number of spatial streams (layers)

N_t : number of antennas

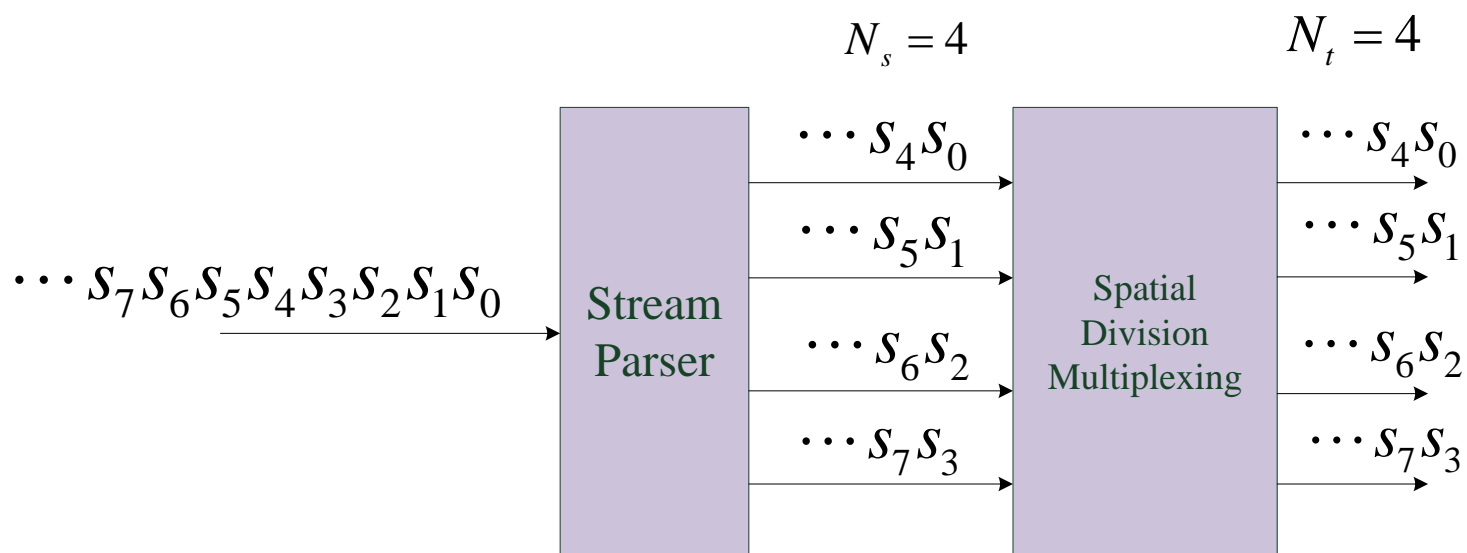
- ◆ There are different MIMO Techniques applied to the multiple layers of data streams
 - ◆ Spatial Division Multiplexing (SDM)
 - ◆ Space-Time Block Coding
 - ◆ Precoding





The MIMO Techniques (2/4)

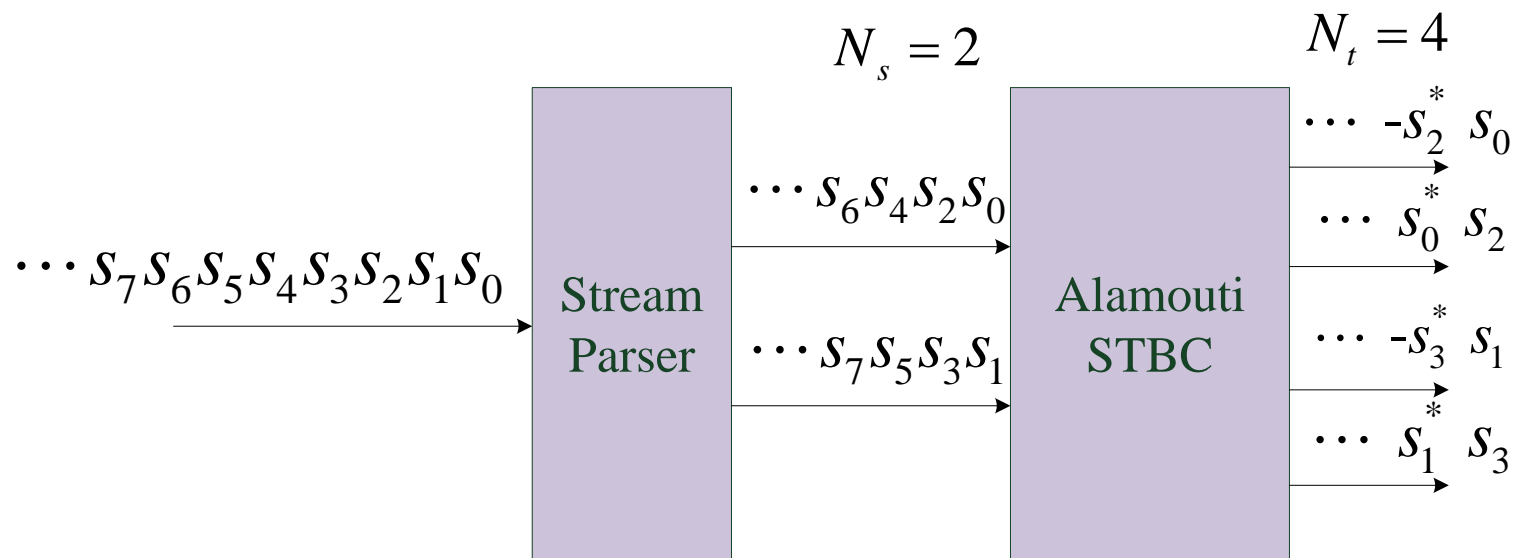
Spatial Division Multiplexing (SDM) MIMO Technique ($N_t = N_s$)



The MIMO Techniques (3/4)



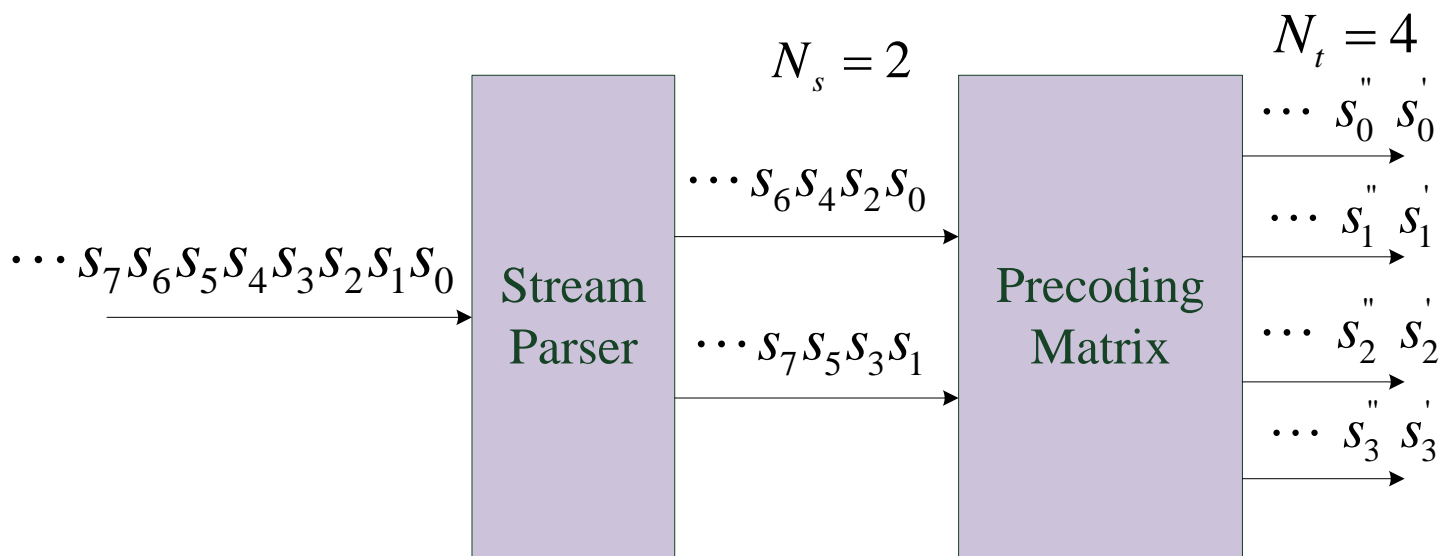
Space Time Block Coding (STBC) MIMO Technique ($N_t > N_s$)



The MIMO Techniques (4/4)

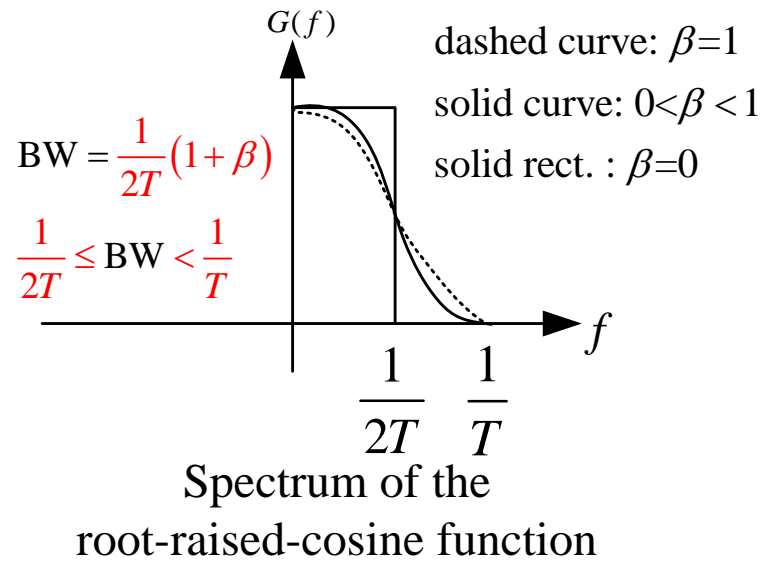
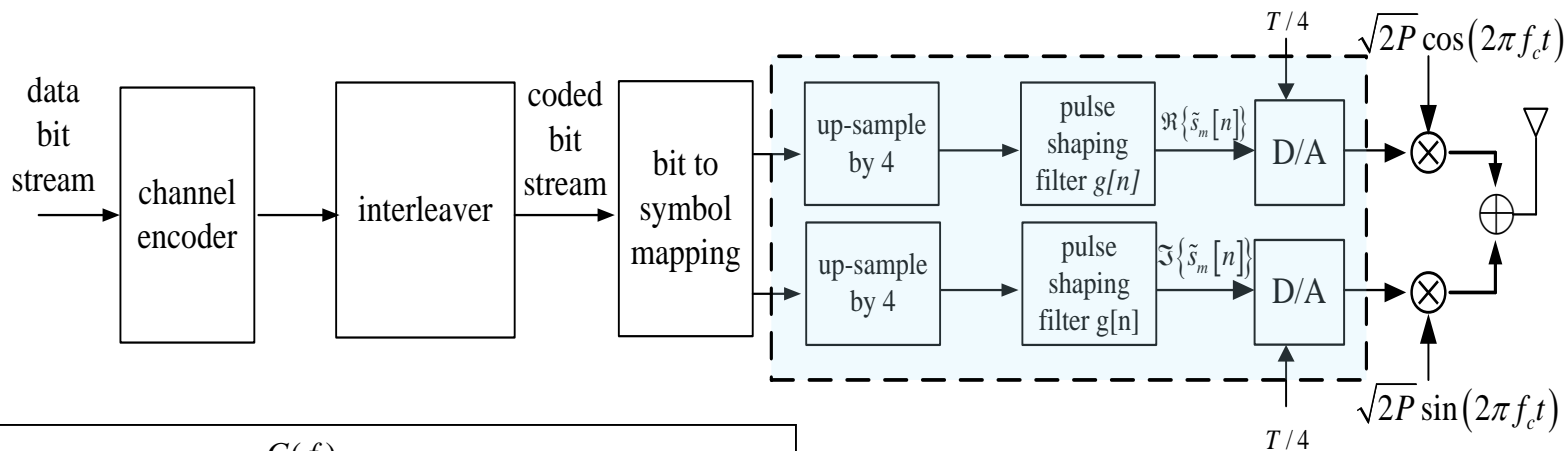


Precoded MIMO Technique ($N_t > N_s$)

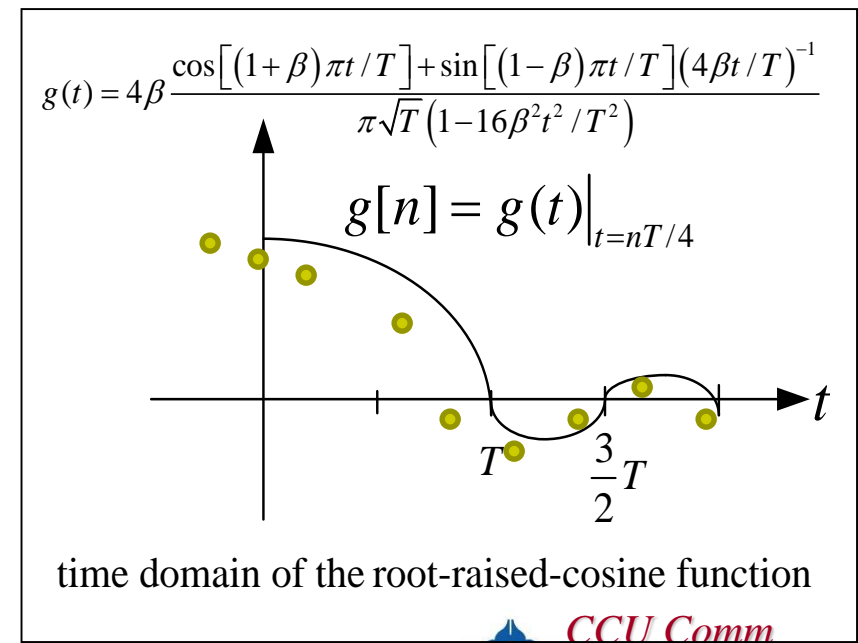




Single Carrier Communication System

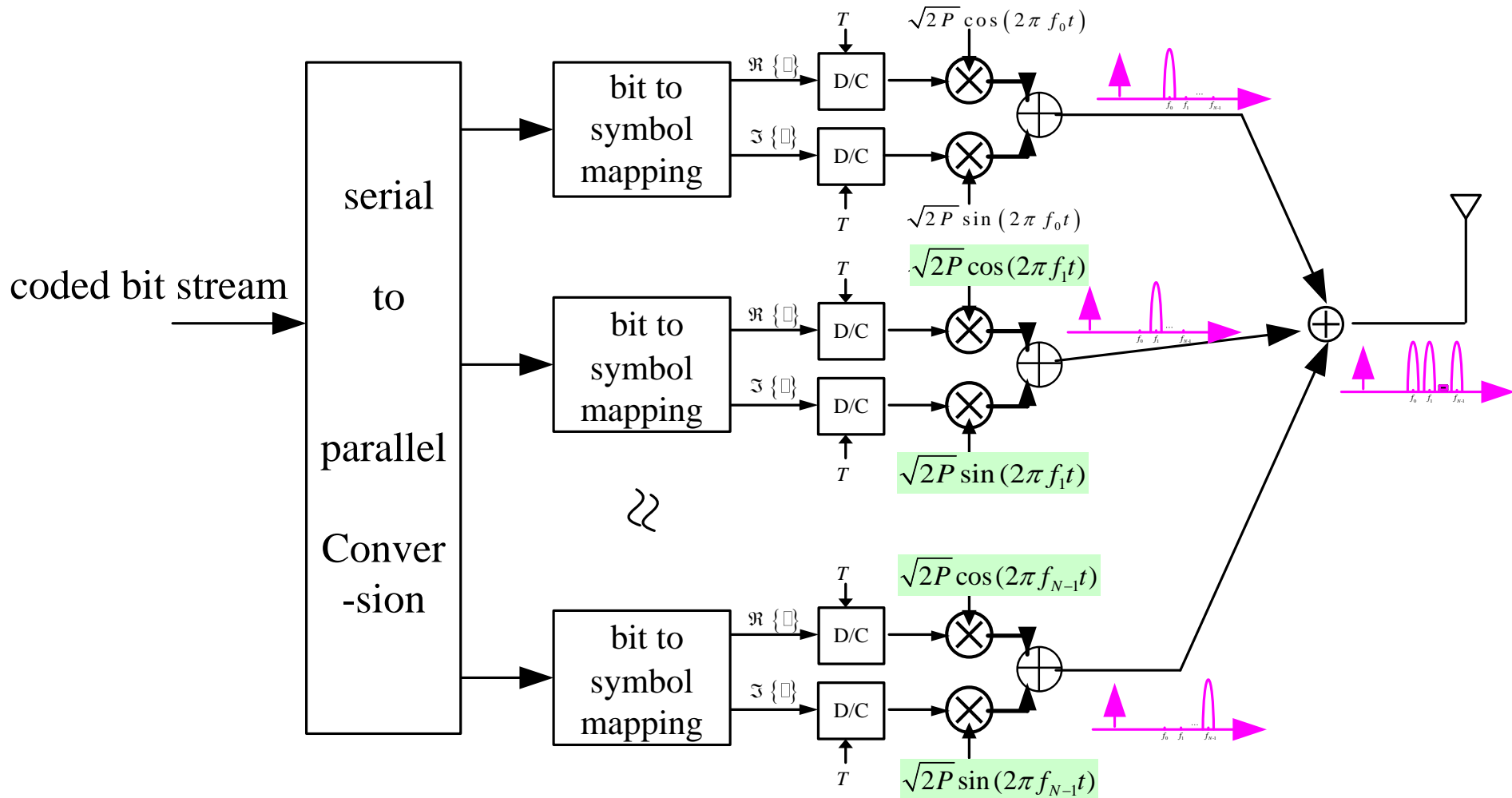


$$\text{Baseband bandwidth } \frac{1+\beta}{2T}$$





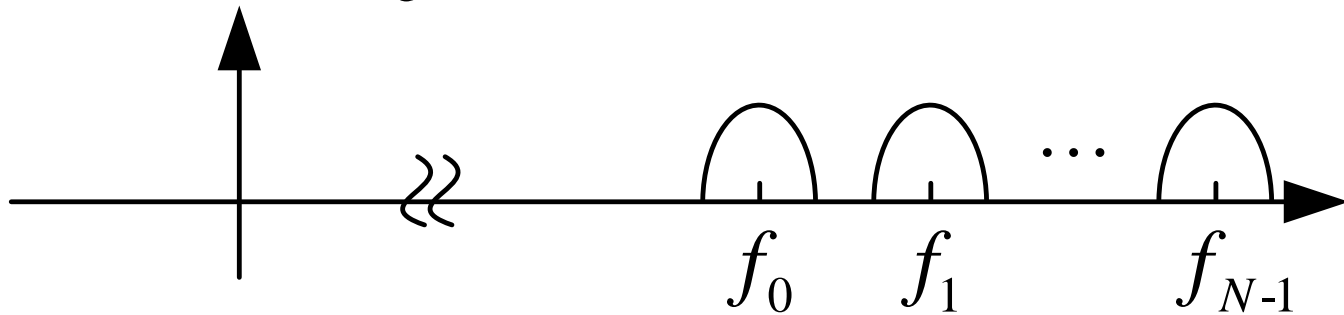
Multi-Carrier Communication System (1/2)



Multi-Carrier Communication System (2/2)

- ◆ If the $f_k, \forall k$, are far apart, the spectrum of the transmitted signal looks as follows.

Spectrum of the multi-carrier modulated signal



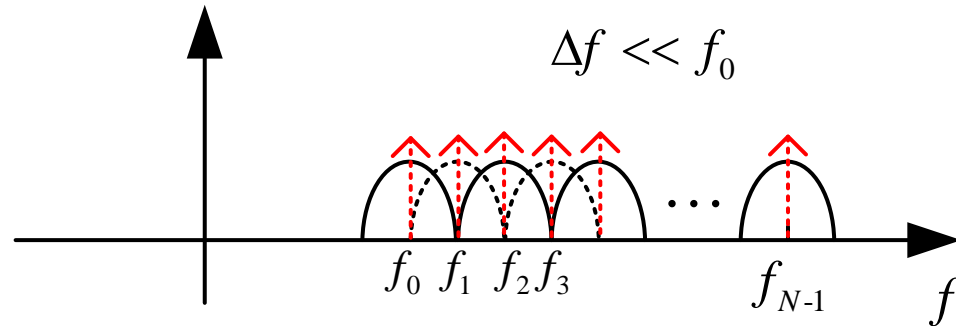
- ◆ The carrier frequencies $f_k, \forall k$, are selected to **avoid spectrum overlapping** such that modulated signals associated with all carriers do not interfere with one another.



The OFDM System (1/5)

- ◆ However, if the carrier frequencies satisfy $f_k = f_0 + k\Delta f$, $k = 0, \dots, N-1$ where f_0 and $\Delta f = \frac{1}{T}$ are fixed values, the spectrum looks like

The spectrum of all multiple carrier modulated signals



The spectra of all multiple sub-signals are overlapped.

It appears that the multiple sub-signals may interfere with one another.

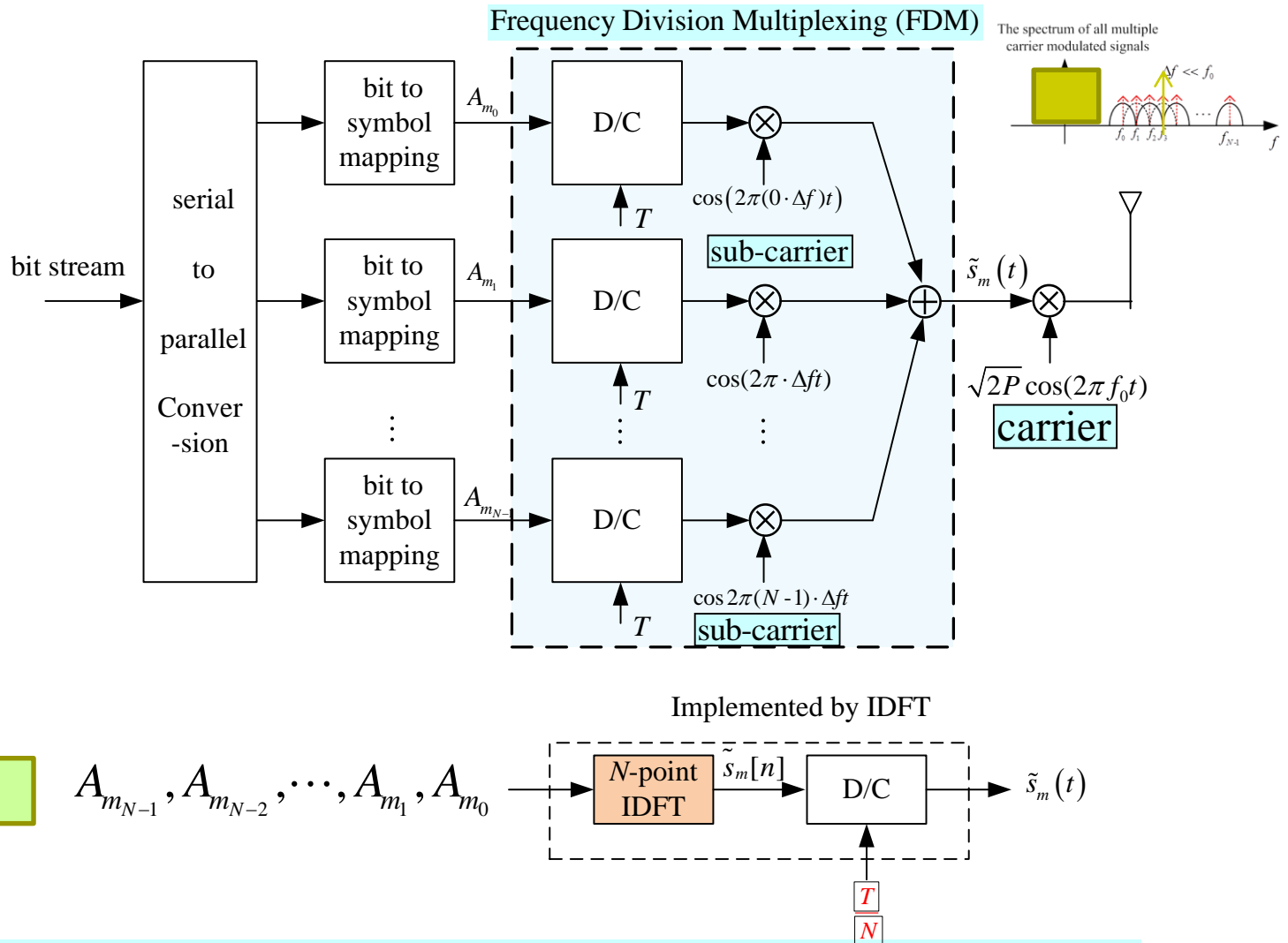
However, the frequency components at frequency instants $f_k = f_0 + k\Delta f, \forall k$, do not interfere with one another.

Through precise frequency synchronization, the receiver can obtain through accurate sampling the frequency components at these frequency instants.

Hence, transmitting signal by this scheme requires accurate frequency synchronization. mm
smart antenna Lab



The OFDM System (2/5)



The N sub-carriers $\{\cos(0\lfloor 2\pi\Delta f t), \cos(1\lfloor 2\pi\Delta f t), \dots, \cos((N-1)\lfloor 2\pi\Delta f t)\}$ are orthogonal.

JCU Comm

The IDFT in OFDM plays **digitally** the role of FDM as in the multi-carrier communication system.

ab



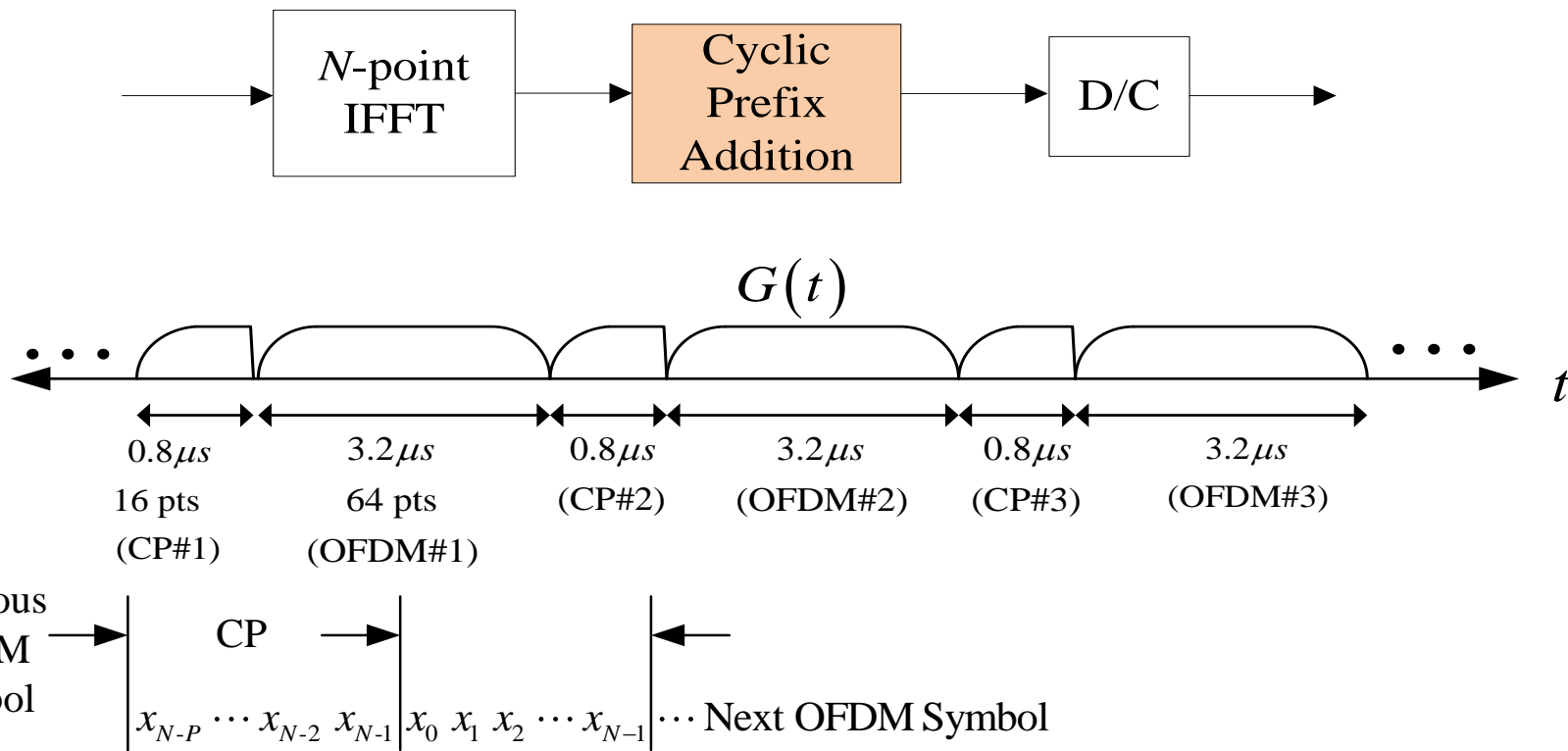
The OFDM System (3/5)

- ◆ The OFDM system is a structure of **Orthogonal FDM** of N parallel signal streams.
- ◆ Advantages of the OFDM system over the multi-carrier (MC)-system:
 - High spectral efficiency (two-fold)
 - Low-complexity (1-tapped) channel equalization
 - Only one RF chain (one mixer/power amplifier, one high-speed DAC)
 - Cheap and stable digital FFT to implement the Orthogonal FDM





The OFDM System (4/5)



One OFDM symbol may include:

N symbols (data in frequency domain)

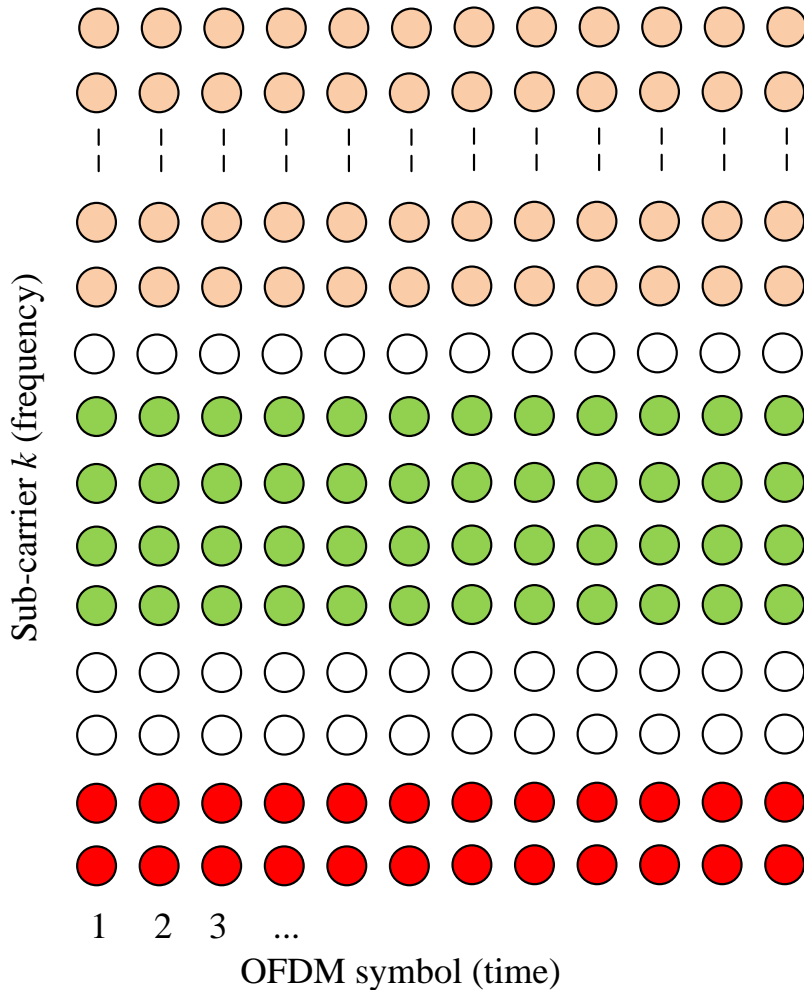
N samples (IFFT size in both time and frequency domains)

$N + P$ samples (IFFT size plus CP length in time domain)





The OFDM System (5/5)



Orthogonal
Frequency Division
Multiple Access
(OFDMA)

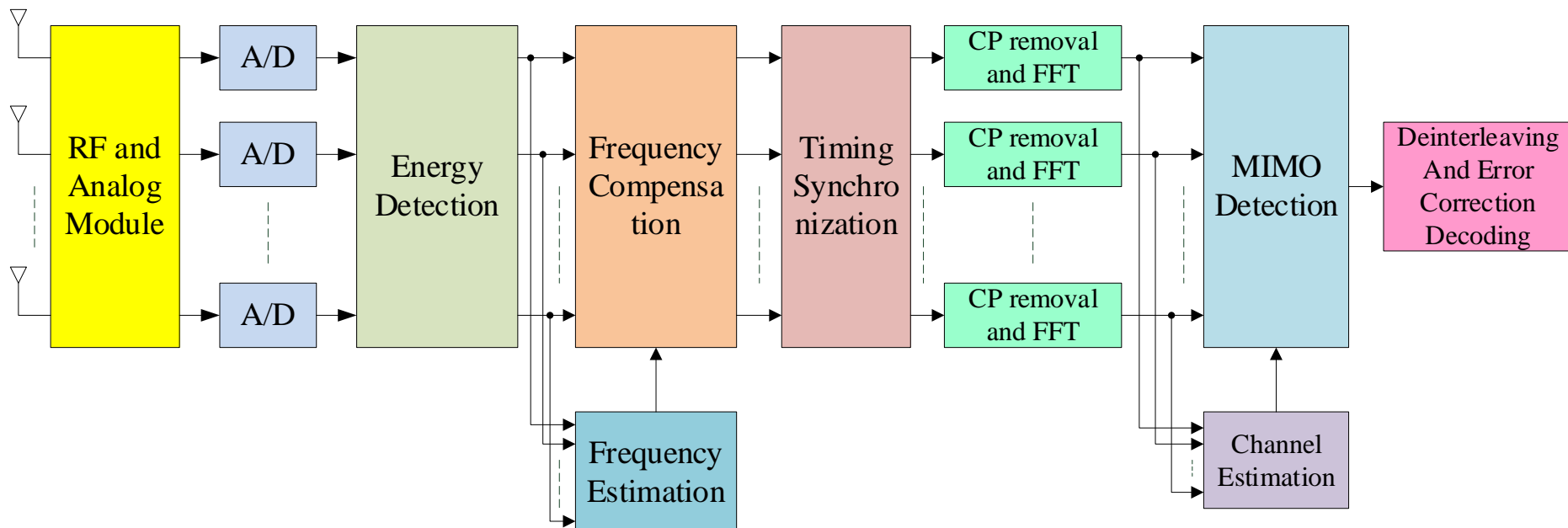
Each user is allocated
with a fixed number
of sub-carriers



MIMO-OFDM Receiver



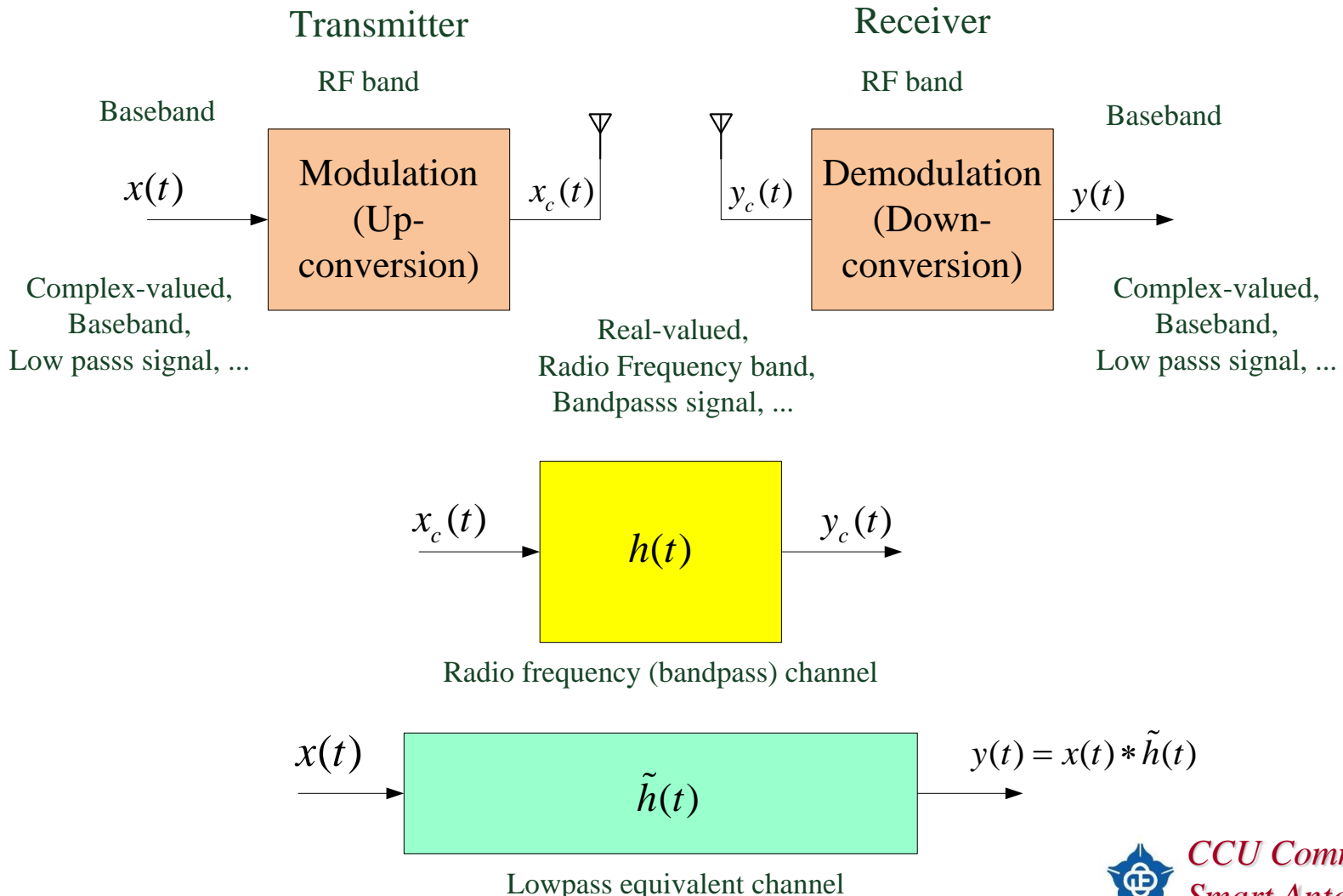
Baseband and Radio Frequency Band Receiver





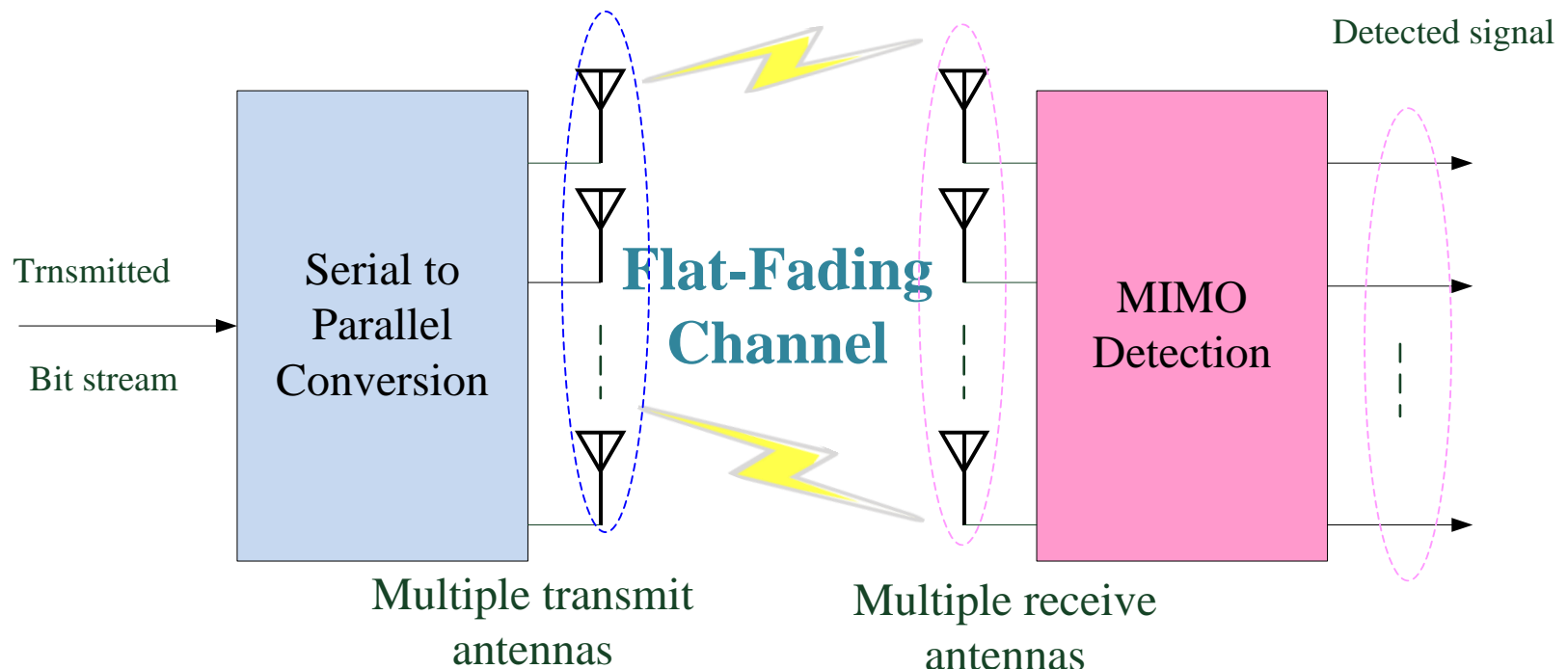
Bandpass Signal and Its Lowpass Representation

$$x_c(t) = A_c \operatorname{Re}\{x(t)\} \cos(2\pi f_c t) + A_c \operatorname{Im}\{x(t)\} \sin(2\pi f_c t)$$





The MIMO System



$$\begin{bmatrix} x_1 \\ x_2 \\ \vdots \\ x_{N_r} \end{bmatrix} = \begin{bmatrix} h_{11} & h_{12} & \cdots & h_{1N_t} \\ h_{21} & h_{22} & \cdots & h_{2N_t} \\ \vdots & \vdots & \ddots & \vdots \\ h_{N_r1} & h_{N_r2} & \cdots & h_{N_rN_t} \end{bmatrix} \begin{bmatrix} s_1 \\ s_2 \\ \vdots \\ s_{N_t} \end{bmatrix} + \begin{bmatrix} w_1 \\ w_2 \\ \vdots \\ w_{N_r} \end{bmatrix}$$

\mathbf{x} \mathbf{H} \mathbf{s} \mathbf{w}





MIMO-OFDM System

The received baseband signal at **sub-carrier k** is

$$\mathbf{x}_k = \mathbf{H}_k \mathbf{P}_k \mathbf{s}_k + \mathbf{w}_k$$

where

\mathbf{x}_k of size $N_r \times 1$ is the received signal

\mathbf{H}_k of size $N_r \times N_t$ is the channel matrix

\mathbf{P}_k of size $N_t \times N_s$ is related to the different MIMO techniques

\mathbf{s}_k of size $N_s \times 1$ is the transmitted symbols at all layers

\mathbf{w}_k of size $N_r \times 1$ is the additive white Gaussian noise





Maximum Likelihood Detection

The MLD of \mathbf{s}_k , $\forall k$, is expressed as

$$\hat{\mathbf{s}}_k = \arg \min_{\mathbf{s}_k \in C^{N_a}} \|\mathbf{x}_k - \mathbf{H}_k \mathbf{P}_k \mathbf{s}_k\|^2$$

where

C denotes the set of symbol constellations.

For the SDM MIMO transmission, $\mathbf{P}_k = \mathbf{I}_k$.

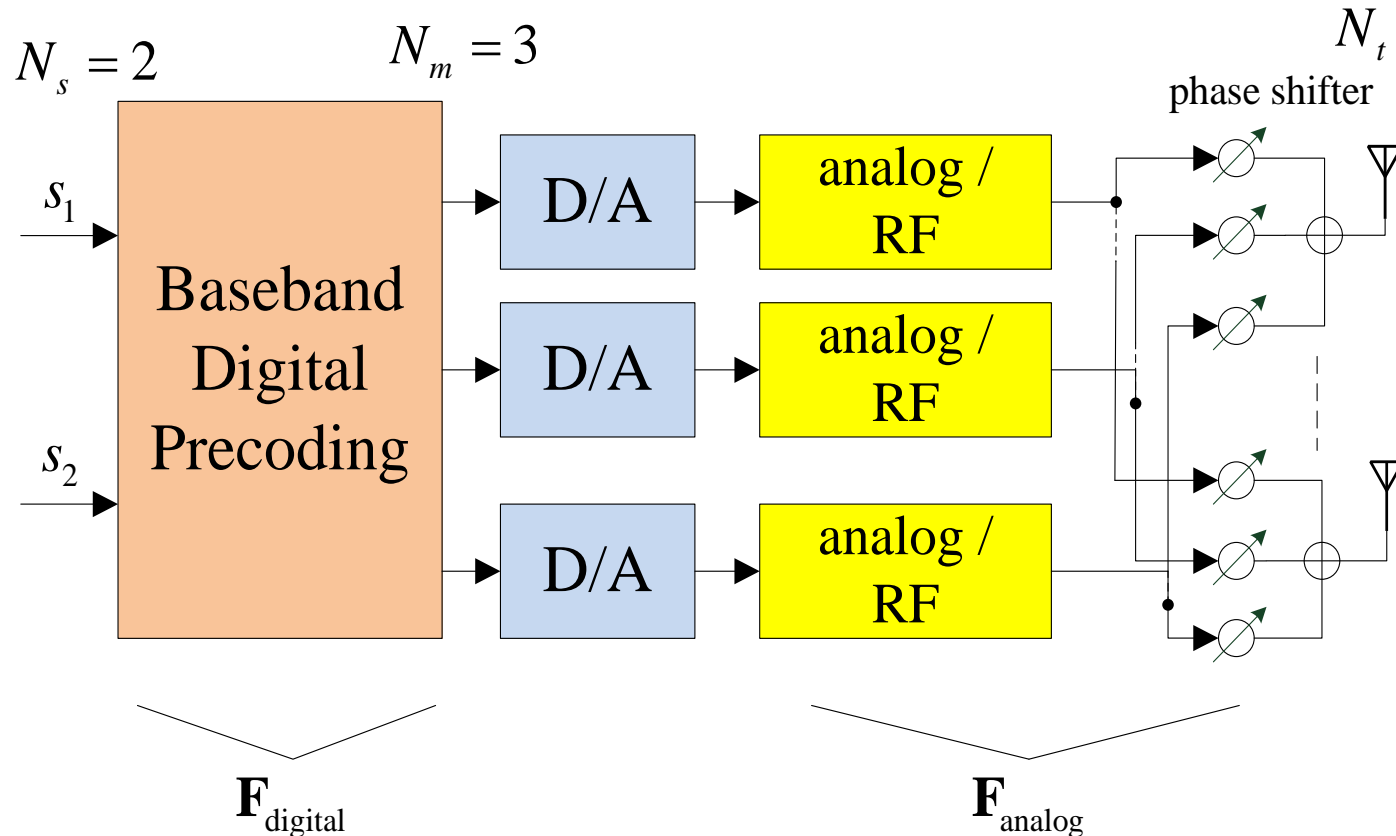
If $\mathbf{H}_k = \mathbf{Q}_k \mathbf{R}_k$ and $\mathbf{y}_k = \mathbf{Q}_k \mathbf{x}_k$ is available,

the MLD becomes

$$\hat{\mathbf{s}}_k = \arg \min_{\mathbf{s}_k \in C^{N_a}} \|\mathbf{y}_k - \mathbf{R}_k \mathbf{s}_k\|^2.$$

Computationally efficient tree search schemes can be applied to obtain $\hat{\mathbf{s}}_k$.

Hybrid Precoding for Millimeter Wave Communications



$$\mathbf{y} = \mathbf{W} \mathbf{H} \mathbf{F} \mathbf{s} + \mathbf{v}$$

$\mathbf{F} = \mathbf{F}_{\text{analog}} \mathbf{F}_{\text{digital}}$ is the precoding matrix.

\mathbf{W} is the combining matrix.

$$N_r \times N_s$$



Part II : CORDIC Rotation and Its Application

- Fundamentals of CORDIC rotation
- QR-Decomposition of Matrices
- QR-Decomposition of Matrices for STBC MIMO System



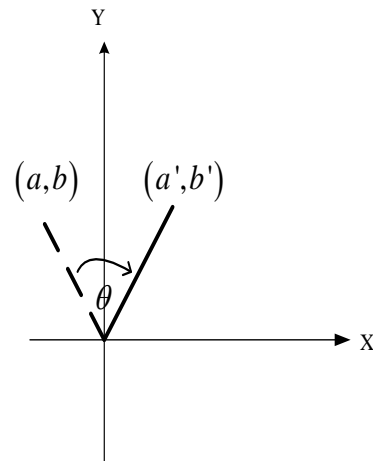


The Givens Rotation

The Givens rotation is used to rotate
a real-valued 2-by-1 vector

$$\begin{bmatrix} a \\ b \end{bmatrix} = \begin{bmatrix} \cos(\theta) & -\sin(\theta) \\ \sin(\theta) & \cos(\theta) \end{bmatrix} \begin{bmatrix} a \\ b \end{bmatrix}$$

or a complex-valued $a + jb$.





CORDIC Algorithm (1/4)

$$\begin{aligned}
 \begin{bmatrix} a' \\ b' \end{bmatrix} &= \begin{bmatrix} \cos \theta & -\sin \theta \\ \sin \theta & \cos \theta \end{bmatrix} \begin{bmatrix} a \\ b \end{bmatrix} \\
 &= \prod_i \begin{bmatrix} \cos \theta_i & -\sin \theta_i \\ \sin \theta_i & \cos \theta_i \end{bmatrix} \begin{bmatrix} a \\ b \end{bmatrix}, \quad \theta = \sum_i \theta_i \\
 &= \left\{ \prod_i \cos \theta_i \right\} \prod_i \begin{bmatrix} 1 & -\tan \theta_i \\ \tan \theta_i & 1 \end{bmatrix} \begin{bmatrix} a \\ b \end{bmatrix}, \quad \text{提出 } \cos \theta_i, \text{ 令 } \tan \theta_i = \pm 2^{-i} \\
 &\approx \left\{ \prod_i \cos(\tan^{-1} 2^{-i}) \right\} \prod_i \begin{bmatrix} 1 & -\sigma_i 2^{-i} \\ \sigma_i 2^{-i} & 1 \end{bmatrix} \begin{bmatrix} a \\ b \end{bmatrix}, \quad \sigma_i = \pm 1 \\
 &= K_n \cdot \prod_i \begin{bmatrix} 1 & -\sigma_i 2^{-i} \\ \sigma_i 2^{-i} & 1 \end{bmatrix} \begin{bmatrix} a \\ b \end{bmatrix}, \quad i \text{ 值夠大時, } K_n = 0.6073
 \end{aligned}$$

$$\theta = \sum_i (\sigma_i \theta_i) = \pm 45^\circ \pm 26.56^\circ \pm 14.04^\circ \pm 7.13^\circ \pm 3.58^\circ \pm 1.79^\circ \pm \dots$$





CORDIC Algorithm (2/4)

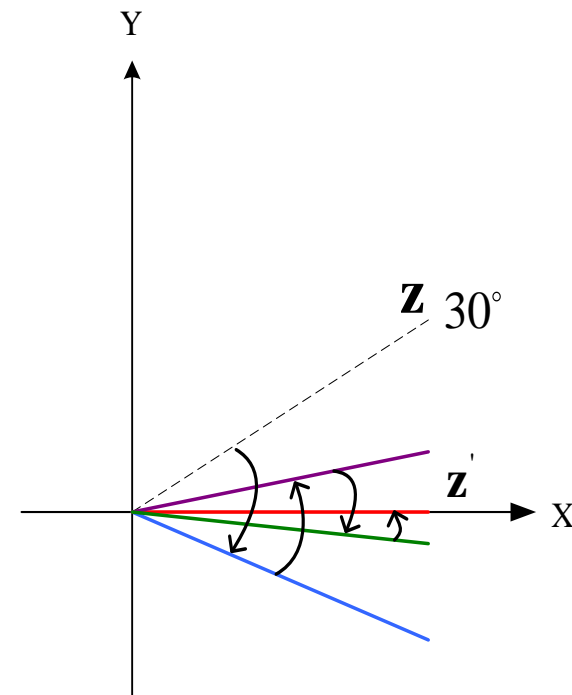
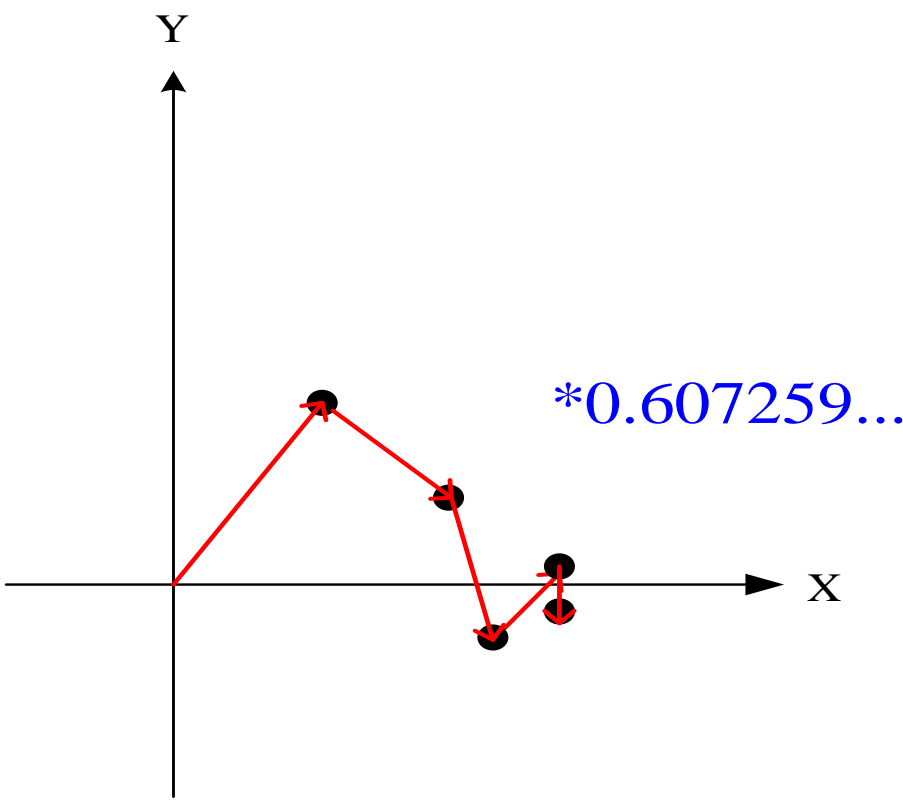
The rotation is decomposed into micro-rotations

$$\theta_i = \tan^{-1}(2^{-i}), i = 0, 1, 2, \dots$$

In practice, only a finite number of micro-rotations is applied.

$$-99.88^\circ \leq \sum_i \theta_i \leq 99.88^\circ$$

$$\theta \approx \sum_i \pm \theta_i = \pm 45^\circ \pm 26.56^\circ \pm 14.04^\circ \pm 7.13^\circ \pm 3.58^\circ \pm 1.79^\circ \pm \dots$$

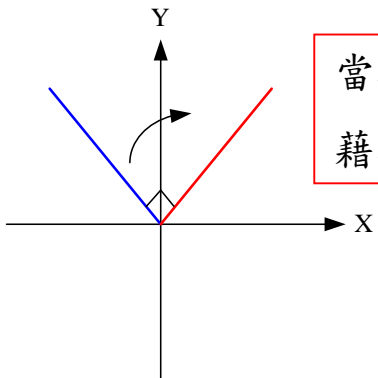




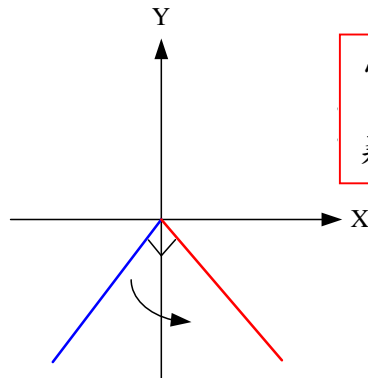
CORDIC Algorithm (3/4)

CORDIC 演算法分成兩種不同的操作模式：Vectoring Mode (VM) 和 Rotation Mode (RM)

Vectoring Mode - Initialization in CORDIC

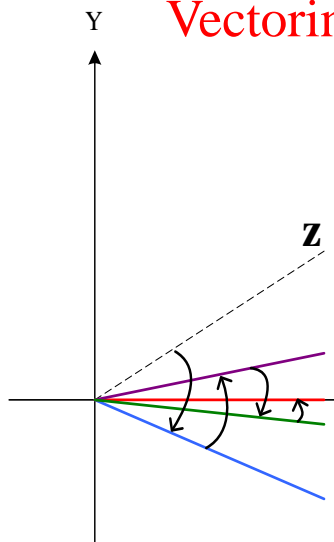


當輸入向量位於第二象限，
藉初始化移動到第一象限上



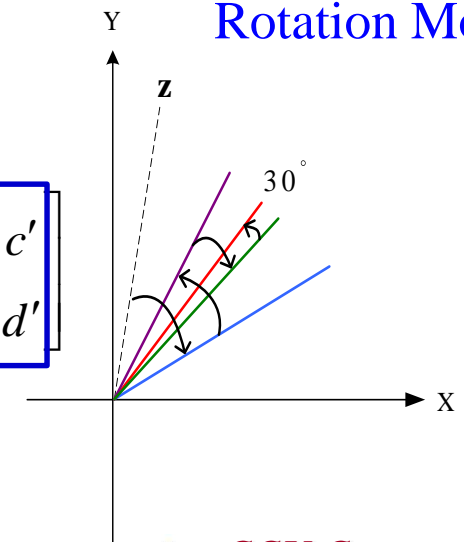
當輸入向量位於第三象限，
藉初始化移動到第四象限上

Vectoring Mode



$$\begin{bmatrix} \cos \theta_{ab} & \sin \theta_{ab} \\ -\sin \theta_{ab} & \cos \theta_{ab} \end{bmatrix} \begin{bmatrix} a & c \\ b & d \end{bmatrix} = \begin{bmatrix} \sqrt{|a|^2 + |b|^2} & 0 \\ c' & d' \end{bmatrix}$$

Rotation Mode





CORDIC Algorithm (4/4)

傳統的CORDIC Vectoring Mode 演算法

Input : $x_{in} + j \cdot y_{in}$

Output : $x_n + j \cdot y_n$, ϕ

% pre-rotation

1. $\sigma_x = sign(x_{in})$

2. $\sigma_y = sign(y_{in})$

3. if $\sigma_x \geq 0$

4. $x_0 = x_{in}$

5. $y_0 = x_{in}$

6. $\omega_0 = 0$

7. else

8. $x_0 = \sigma_y \cdot y_{in}$

9. $y_0 = -\sigma_y \cdot x_{in}$

10. $\omega_0 = 0 + \sigma_y \cdot \alpha_{-1}$

11. end

% end pre-rotation

12. for $i = 0 : n - 1$, do

13. $\sigma_i = sign(y_i)$

14. $x_{i+1} = x_i + \sigma_i \cdot 2^{-i} \cdot y_i$

15. $y_{i+1} = y_i - \sigma_i \cdot 2^{-i} \cdot x_i$

16. $\omega_{i+1} = \omega_i + \sigma_i \cdot \alpha_i$

17. end

18. $\phi = \omega_n$

look-up-table free 之 CORDIC Vectoring Mode 演算法

Input : $x_{in} + j \cdot y_{in}$

Output : $x_n + j \cdot y_n$

$\sigma_x, \sigma_y, \sigma = [\sigma_0 \ \sigma_1 \ \dots \ \sigma_i \ \dots \ \sigma_{n-1}]$

% pre-rotation

1. $\sigma_x = sign(x_{in})$

2. $\sigma_y = sign(y_{in})$

3. if $\sigma_x \geq 0$

4. $x_0 = x_{in}$

5. $y_0 = x_{in}$

6. else

7. $x_0 = \sigma_y \cdot y_{in}$

8. $y_0 = -\sigma_y \cdot x_{in}$

9. end

% end pre-rotation

10. for $i = 0 : n - 1$, do

11. $\sigma_i = sign(y_i)$

12. $x_{i+1} = x_i + \sigma_i \cdot 2^{-i} \cdot y_i$

13. $y_{i+1} = y_i - \sigma_i \cdot 2^{-i} \cdot x_i$

14. end

傳統的CORDIC Rotation Mode 演算法

Input : $x_{in} + j \cdot y_{in}$, ω_{in}

Output : $x_n + j \cdot y_n$

% pre-rotation

1. if $-\alpha_{-1} \geq \omega_{in} \geq \alpha_{-1}$

2. $x_0 = x_{in}$

3. $y_0 = x_{in}$

4. $\omega_0 = \omega_{in}$

5. else

6. $\sigma_\omega = -sign(\omega_{in})$

7. $x_0 = \sigma_\omega \cdot y_{in}$

8. $y_0 = -\sigma_\omega \cdot x_{in}$

9. $\omega_0 = \omega_{in} + \sigma_\omega \cdot \alpha_{-1}$

10. end

% end pre-rotation

10. for $i = 0 : n - 1$, do

11. $\sigma_i = -sign(\omega_i)$

12. $x_{i+1} = x_i + \sigma_i \cdot 2^{-i} \cdot y_i$

13. $y_{i+1} = y_i - \sigma_i \cdot 2^{-i} \cdot x_i$

14. $\omega_{i+1} = \omega_i + \sigma_i \cdot \alpha_i$

15. end

look-up-table free 之 CORDIC Rotation Mode 演算法

Input : $x_{in} + j \cdot y_{in}$

$\sigma_x, \sigma_y, \sigma = [\sigma_0 \ \sigma_1 \ \dots \ \sigma_i \ \dots \ \sigma_{n-1}]$

Output : $x_n + j \cdot y_n$

% pre-rotation

1. if $\sigma_x \geq 0$

2. $x_0 = x_{in}$

3. $y_0 = x_{in}$

4. else

5. $x_0 = \sigma_y \cdot y_{in}$

6. $y_0 = -\sigma_y \cdot x_{in}$

7. end

% end pre-rotation

8. for $i = 0 : n - 1$, do

9. $x_{i+1} = x_i + \sigma_i \cdot 2^{-i} \cdot y_i$

10. $y_{i+1} = y_i - \sigma_i \cdot 2^{-i} \cdot x_i$

11. end





Real-Valued Givens Rotation

For real-valued $\begin{bmatrix} a & c \\ b & d \end{bmatrix}$,

$$\begin{bmatrix} \cos(\theta_{ab}) & -\sin(\theta_{ab}) \\ \sin(\theta_{ab}) & \cos(\theta_{ab}) \end{bmatrix} \begin{bmatrix} a & c \\ b & d \end{bmatrix}$$

$$= \begin{bmatrix} \sqrt{|a|^2 + |b|^2} & c' \\ 0 & d' \end{bmatrix}$$

\therefore 1 Givens rotation is used to compute $\sqrt{|a|^2 + |b|^2}$.

\therefore 1 Givens rotation is used to compute (c', d') .

where

$$\theta_{ab} = \tan^{-1}(b/a).$$





Complex-Valued Givens Rotation

For complex-valued $\begin{bmatrix} a & c \\ b & d \end{bmatrix}$,

$$\begin{bmatrix} \cos(\theta_{ab}) & -\sin(\theta_{ab}) \\ \sin(\theta_{ab}) & \cos(\theta_{ab}) \end{bmatrix} \begin{bmatrix} e^{-j\theta_a} & 0 \\ 0 & e^{-j\theta_b} \end{bmatrix} \begin{bmatrix} a & c \\ b & d \end{bmatrix}$$

$$= \begin{bmatrix} \cos(\theta_{ab}) & -\sin(\theta_{ab}) \\ \sin(\theta_{ab}) & \cos(\theta_{ab}) \end{bmatrix} \begin{bmatrix} |a| & c' \\ |b| & d' \end{bmatrix}$$

$$= \begin{bmatrix} \sqrt{|a|^2 + |b|^2} & c'' \\ 0 & d'' \end{bmatrix}$$

where

$$\theta_a = \angle a, \quad \theta_b = \angle b, \quad \text{and} \quad \theta_{ab} = \tan^{-1}(|b|/|a|).$$

\therefore 3 Givens rotations are used to compute $\sqrt{|a|^2 + |b|^2}$.

\therefore 4 Givens rotations are used to compute (c'', d'') .





Part II : CORDIC Rotation and Its Application

- Fundamentals of CORDIC rotation
- QR-Decomposition of Matrices
- QR-Decomposition of Matrices for STBC MIMO System





QR-Decomposition of an m -by- n Matrix

If \mathbf{A} is an $m \times n$ matrix with linearly independent columns, then A can be factored as $\mathbf{A} = \mathbf{Q}\mathbf{R}$, where \mathbf{Q} is an $m \times n$ matrix whose columns from an orthonormal basis for the column space of \mathbf{A} and \mathbf{R} is an $n \times n$ upper triangular invertible matrix with positive entries on its diagonal.

QRD Methods

- Givens rotation based methods
- Gram-Schmidt Orthogonalization
- Householder transformation



QRD of a 3-by3 complex matrix

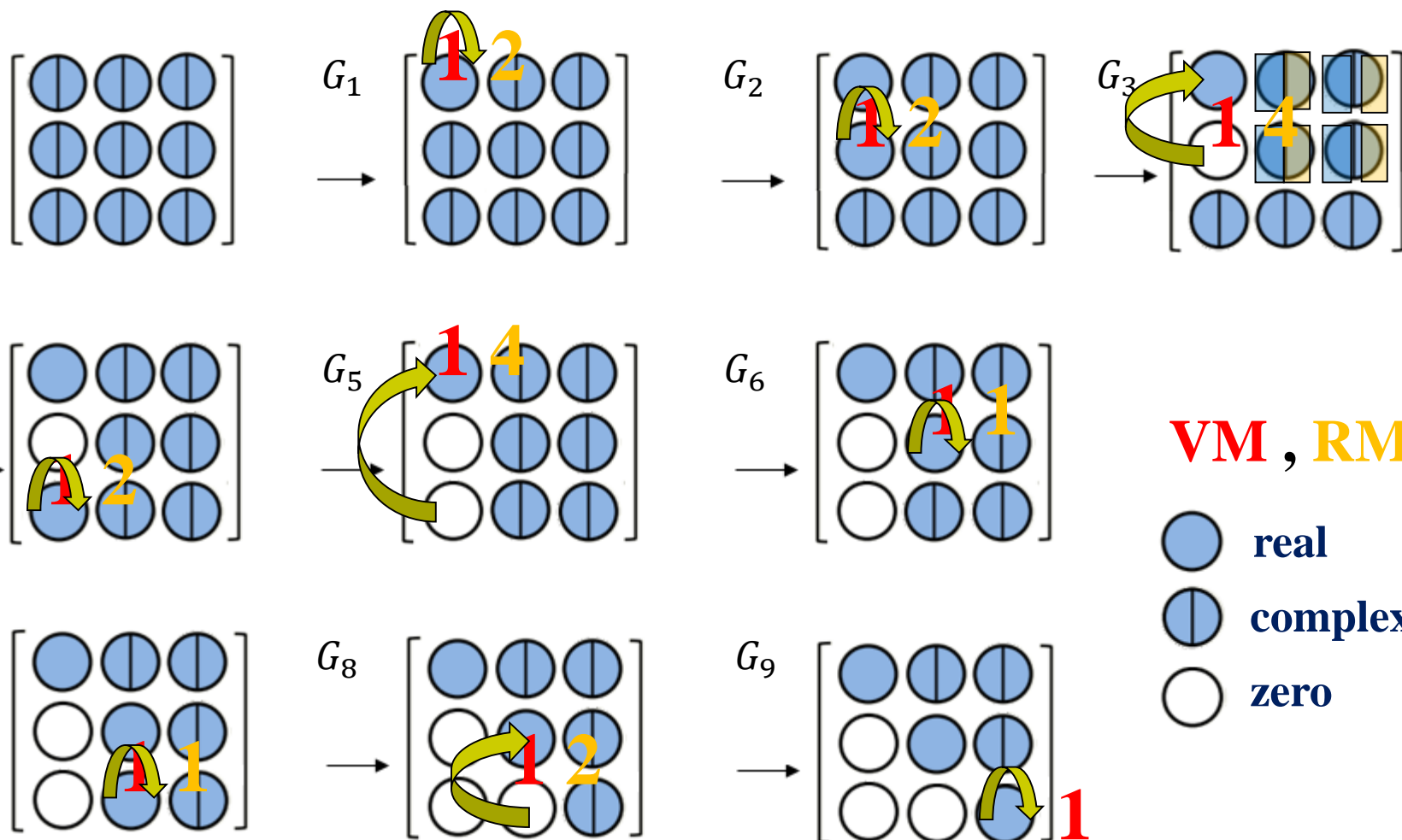
$$\mathbf{G}_9 \mathbf{G}_8 \mathbf{G}_7 \mathbf{G}_6 \mathbf{G}_5 \mathbf{G}_4 \mathbf{G}_3 \mathbf{G}_2 \mathbf{G}_1 \mathbf{H} = \mathbf{R}$$

$$\text{let } \mathbf{G} = \mathbf{G}_9 \mathbf{G}_8 \mathbf{G}_7 \mathbf{G}_6 \mathbf{G}_5 \mathbf{G}_4 \mathbf{G}_3 \mathbf{G}_2 \mathbf{G}_1$$

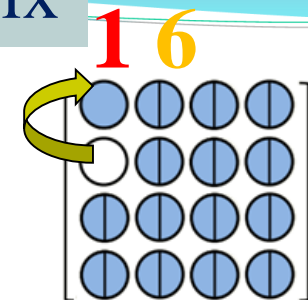
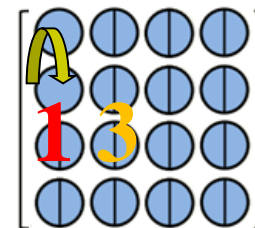
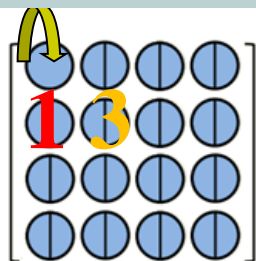
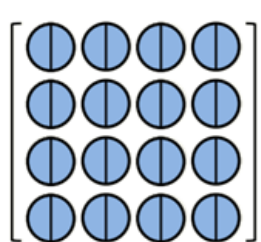
$$\Rightarrow \mathbf{GH} = \mathbf{R}$$

$$\Rightarrow \mathbf{H} = \mathbf{G}^{-1} \mathbf{R} = \mathbf{G}^H \mathbf{R} \quad \Rightarrow \mathbf{H} = \mathbf{QR}$$

 : real part
 : imag part

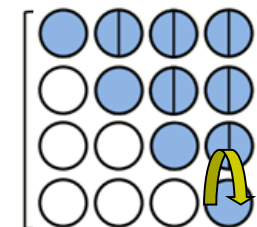
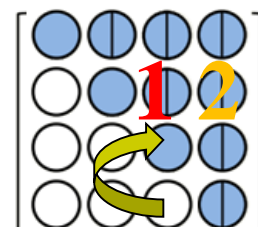
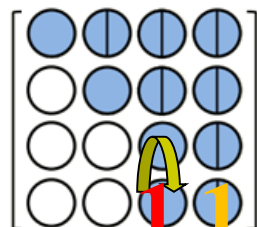
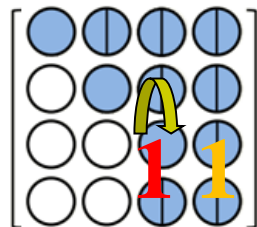
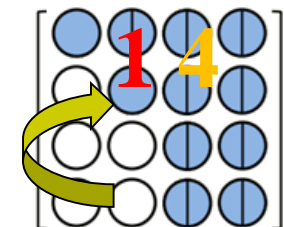
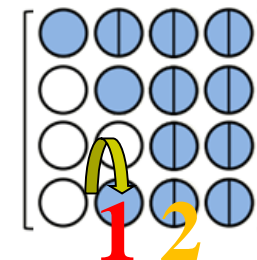
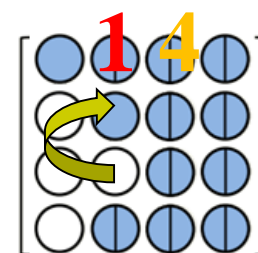
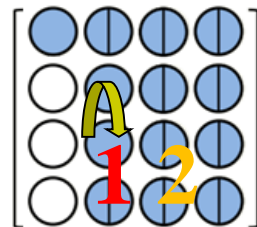
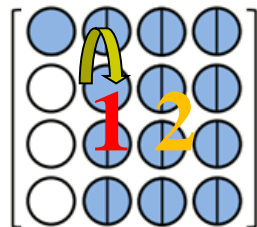
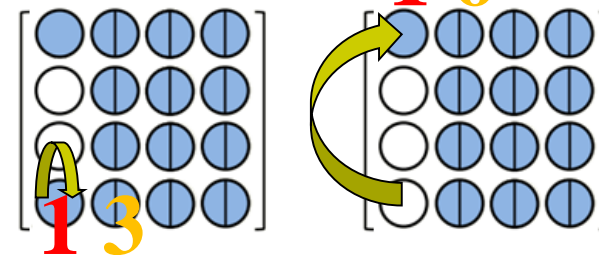
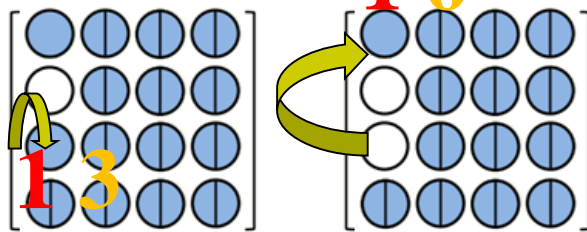


QRD of 4-by-4 complex matrix



VM, **RM**

- real
- complex
- zero





The CORDIC Module

Number of Iteration : 9 times
word length : 14 bits
pipeline : 3 (after the 2nd, 6th, and last multiplication)

VM

for $i = 0 : n - 1$

$$\sigma_i = \text{sign}(y_i)$$

$$x_{i+1} = x_i + \sigma_i \cdot 2^{-i} \cdot y_i$$

$$y_{i+1} = y_i - \sigma_i \cdot 2^{-i} \cdot x_i$$

$$w_{i+1} = w_i + \sigma_i \cdot \alpha_i$$

end

RM

for $i = 0 : n - 1$

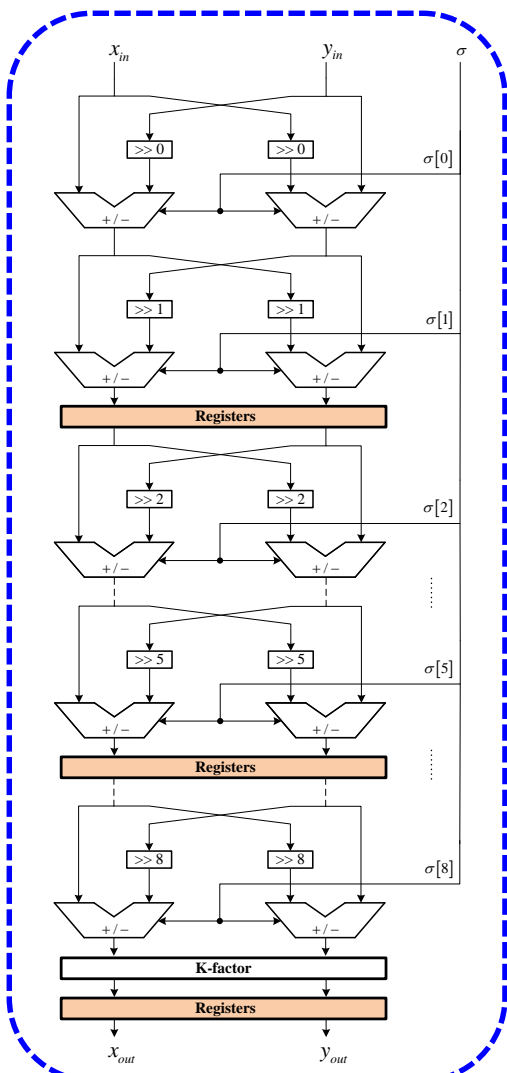
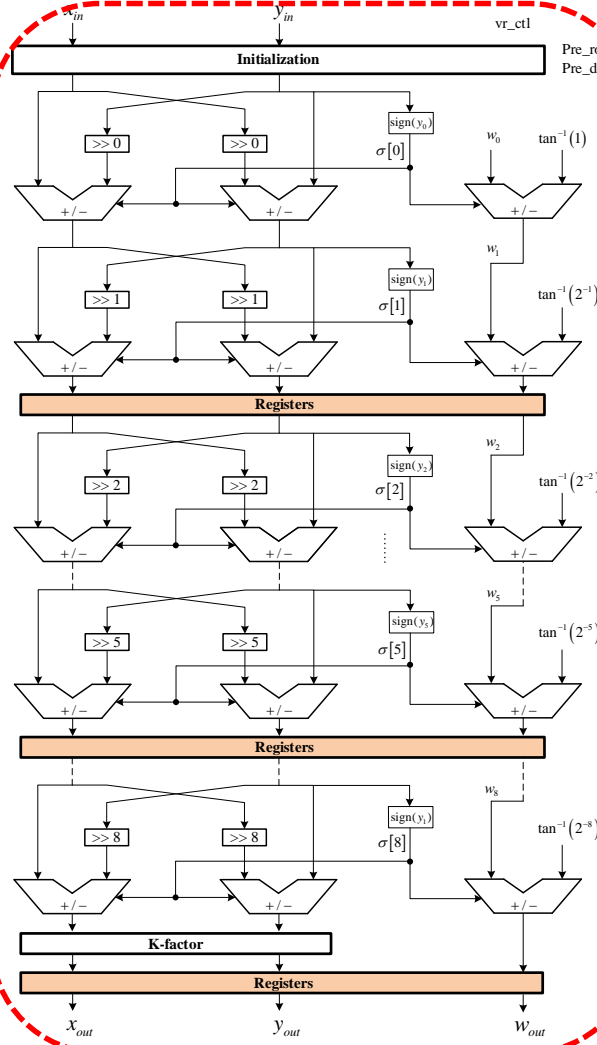
$$\sigma_i = -\text{sign}(w_i)$$

$$x_{i+1} = x_i + \sigma_i \cdot 2^{-i} \cdot y_i$$

$$y_{i+1} = y_i - \sigma_i \cdot 2^{-i} \cdot x_i$$

end

$$\alpha_i = \tan^{-1}(2^{-i})$$



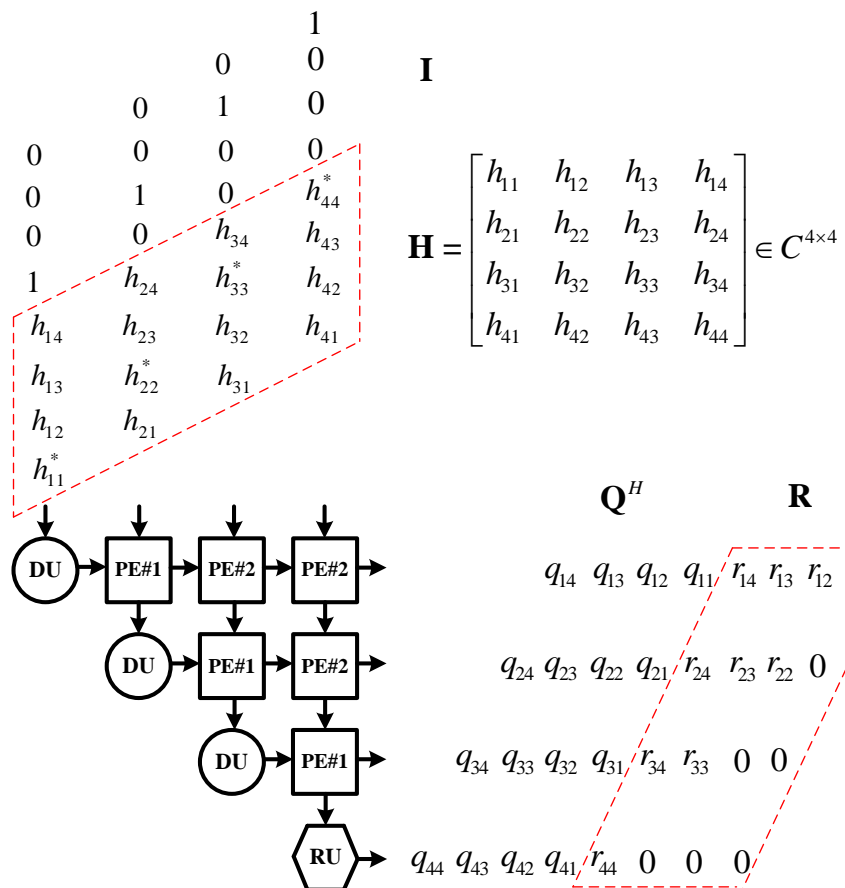
Finite number of micro-rotations





TACR Triangular Systolic Array (1/3)

QR分解 4×4 H通道矩阵之TACR-TSA架構



DU :

Delay Unit, delays the input signal (for period equal to PE operation time).

PE :

Processing Element, may operate in Vectoring and Rotation mode.

RU :

Rotation Unit, eliminates the complex lowest diagonal element of upper triangular matrix R.

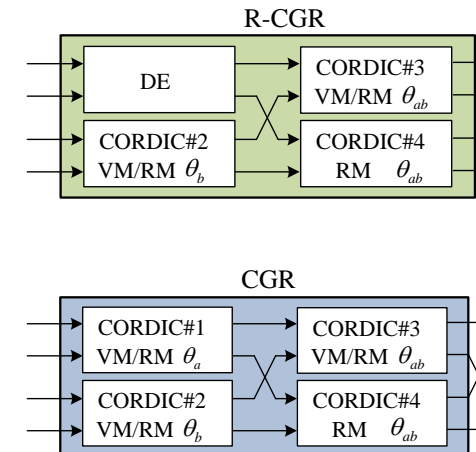
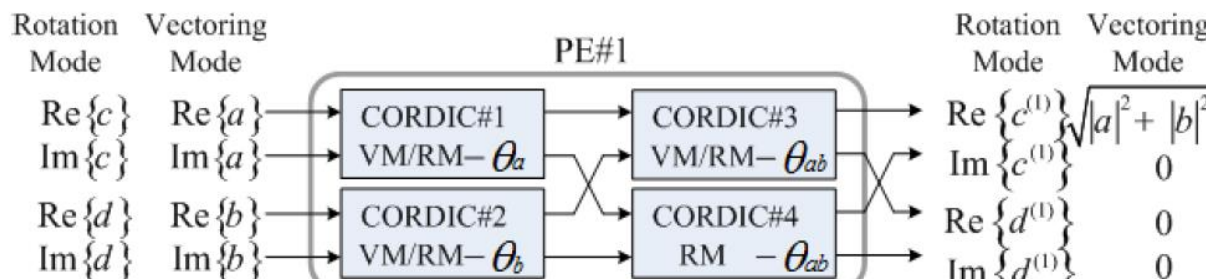
$$\begin{bmatrix} \sqrt{|a|^2 + |b|^2} & c^{(1)} \\ 0 & d^{(1)} \end{bmatrix} = \begin{bmatrix} \cos \theta_{ab} & \sin \theta_{ab} \\ -\sin \theta_{ab} & \cos \theta_{ab} \end{bmatrix} \begin{bmatrix} e^{-j\theta_a} & 0 \\ 0 & e^{-j\theta_b} \end{bmatrix} \begin{bmatrix} a \\ b \\ c \\ d \end{bmatrix}$$



TACR Triangular Systolic Array (2/3)

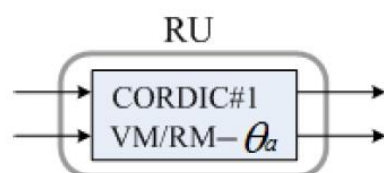
PE :

Processing Element, may operate in Vectoring and Rotation mode.



RU :

Rotation Unit, eliminates the complex lowest diagonal element of upper triangular matrix R.





TACR Triangular Systolic Array (3/3)

時序分析圖

clk	01	02	03	04	05	06	07	08	09	10	11	12	13	14	15	16	17	18	19	20	21	22	23	24	25	26	27	28	29	30	31	32	33	34	35	36	37	38	39	40	41	42
	\	\	\	\	\	\			VH _{11,21}				VH _{11,31}			VH _{11,41}																										
									RH _{12,22}				RH _{12,32}			RH _{12,42}																										
									RH _{13,23}				RH _{13,33}			RH _{13,43}																										
									RH _{14,24}				RH _{14,34}			RH _{14,44}				VH _{22,32}			VH _{22,42}																			
										\	\	\	\	\	\	\	\	\		RH _{23,33}			RH _{23,43}																			
										\	\	\	\	\	\	\	\	\	\	RH _{24,34}			RH _{24,44}																			
																					\	\	\	\	\	\	\	\	\	VH _{33,43}												
																														RH _{34,44}												
																																								VH ₄₄		

其中 $VH_{ij,lk}$ 表示做 TACR VM 操作

$RH_{ij,lk}$ 表示做 TACR RM 操作

最後一個 VH_{jj} 表示做 RU 元件的動作





Hardware Implementation Results

Algorithm	Givens Rotation (CORDIC)
System (Tx-Rx)	SDM-MIMO (4-by-4)
Architecture	TSA
Matrix Size	Complex 4-by-4
Word lengths	16 bits
Iterations	9
Technology	ASIC 90 nm

Frequency	125.4 MHz
Gate Count	132K
Processing Cycles (clock cycles)	8
Processing Latency (clock cycles)	46
Power Consumption (mW)	19 at 0.9V
Energy consumed per QRD (nJ)	1.21
Throughput rate	15.675M matrices/sec

Throughput rate = frequency / processing cycles





Pros and Cons of CORDIC Based Architecture

Advantages	Disadvantages
Fully parallel hardware structure	Long latency
Configurable structure	High bandwidth requirements both for periphery (RAM) and between PEs.
Division free circuits	Poor run-time fault tolerance due to lack of inter-connection protocol.



Part II : CORDIC Rotation and Its Application

- Fundamentals of CORDIC rotation
- QR-Decomposition of Matrices
- QR-Decomposition of Matrices for STBC MIMO System





Alamouti STBC MIMO

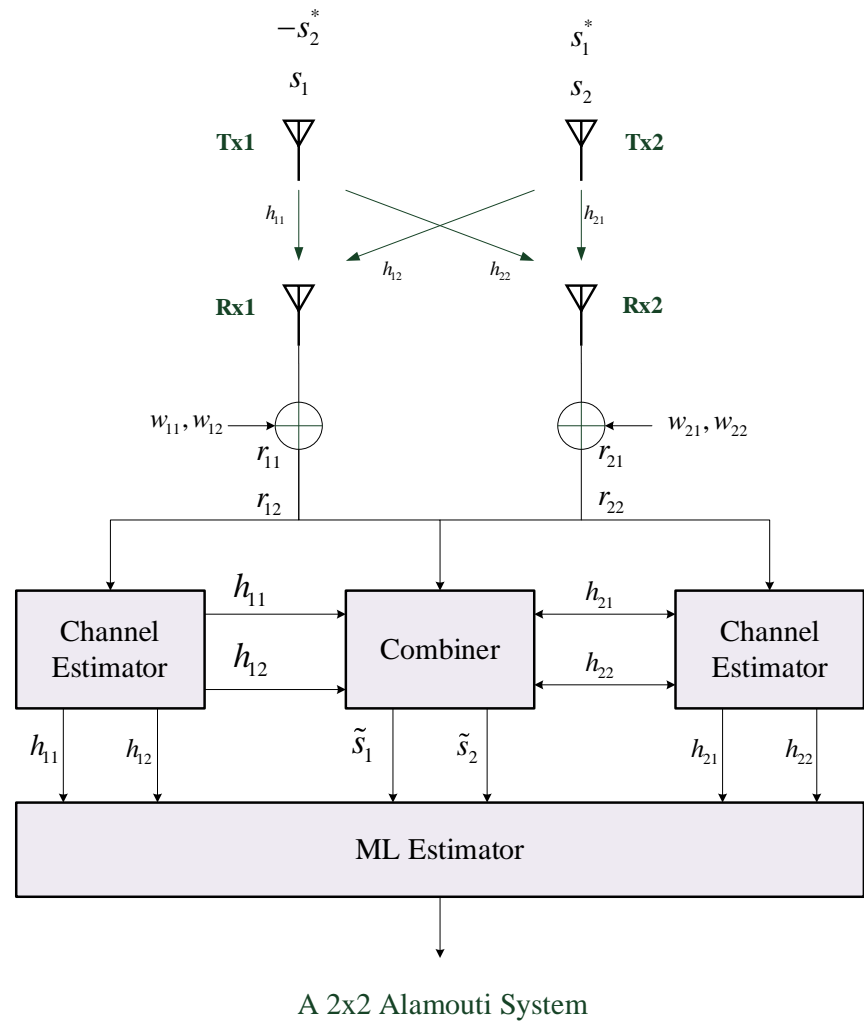
System Model :

$$\begin{bmatrix} x_{1,1} & x_{1,2} \\ x_{2,1} & x_{2,2} \end{bmatrix} = \begin{bmatrix} h_{1,1} & h_{1,2} \\ h_{2,1} & h_{2,2} \end{bmatrix} \begin{bmatrix} s_1 \\ s_2 \end{bmatrix} + \begin{bmatrix} w_{1,1} & w_{1,2} \\ w_{2,1} & w_{2,2} \end{bmatrix}$$

$$\mathbf{S}_m \square \begin{bmatrix} s_{2m-1} & -s_{2m}^* \\ s_{2m} & s_{2m-1}^* \end{bmatrix}$$

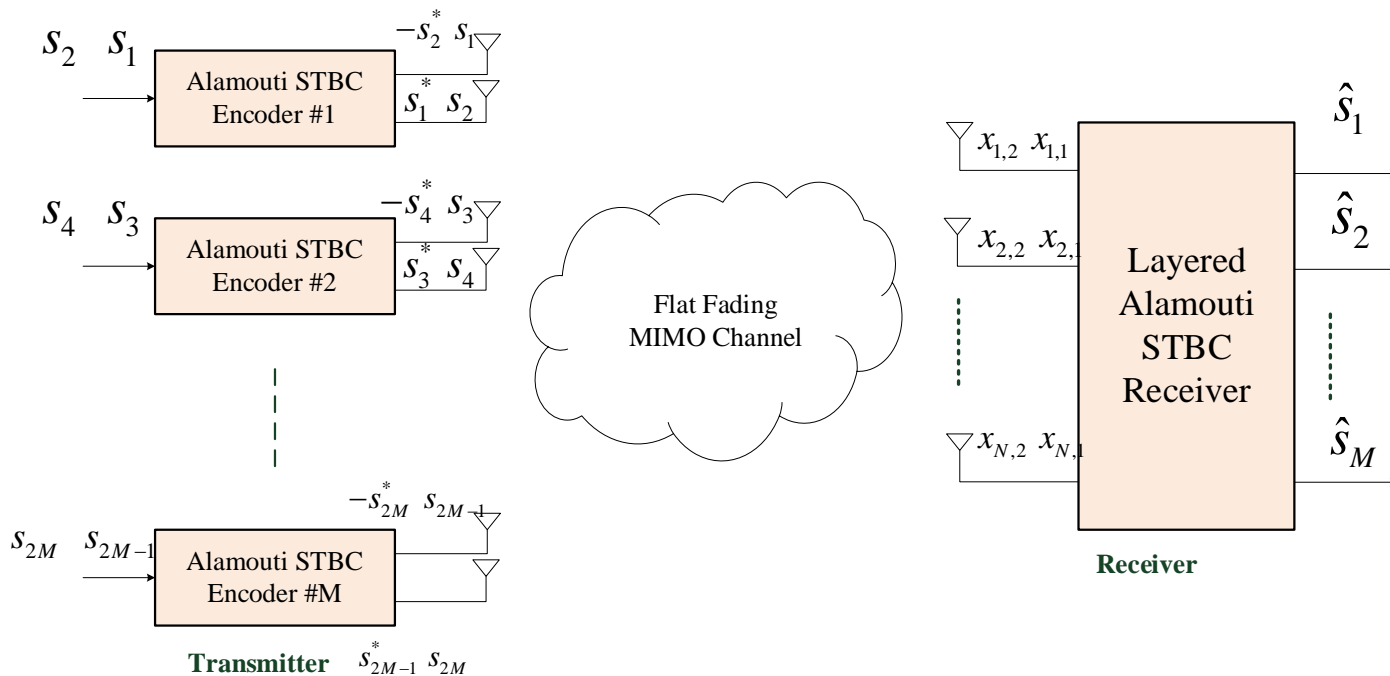
Convert to linear model

$$\begin{bmatrix} x_{1,1} \\ -x_{1,2}^* \\ x_{2,1} \\ -x_{2,2}^* \end{bmatrix} = \underbrace{\begin{bmatrix} h_{1,1} & h_{1,2} \\ -h_{1,2}^* & h_{1,1}^* \\ h_{2,1} & h_{2,2} \\ -h_{2,2}^* & h_{2,1}^* \end{bmatrix}}_{\mathbf{H}} \underbrace{\begin{bmatrix} s_1 \\ s_2 \end{bmatrix}}_{\mathbf{S}} + \underbrace{\begin{bmatrix} w_{1,1} \\ -w_{1,2}^* \\ w_{2,1} \\ -w_{2,2}^* \end{bmatrix}}_{\mathbf{W}}$$





Layered Alamouti STBC MIMO System



System model :

$$\begin{bmatrix} x_{1,1} & x_{1,2} \\ \vdots & \vdots \\ x_{N,1} & x_{N,2} \end{bmatrix} = \begin{bmatrix} h_{1,1} & \cdots & h_{1,2M} \\ \vdots & \ddots & \vdots \\ h_{N,1} & \cdots & h_{N,2M} \end{bmatrix} \begin{bmatrix} \mathbf{S}_1 \\ \vdots \\ \mathbf{S}_M \end{bmatrix} + \mathbf{W}$$

$$\mathbf{S}_m \square \begin{bmatrix} s_{2m-1} & -s_{2m}^* \\ s_{2m} & s_{2m-1}^* \end{bmatrix}$$





Layered Alamouti STBC MIMO System

Convert to linear model

$$\underbrace{\begin{bmatrix} x_{1,1} \\ -x_{1,2}^* \\ \vdots \\ x_{N,1} \\ -x_{N,2}^* \end{bmatrix}}_{\mathbf{x}} = \underbrace{\begin{bmatrix} \mathbf{H}_{1,1} & \cdots & \mathbf{H}_{1,M} \\ \vdots & \ddots & \vdots \\ \mathbf{H}_{N,1} & \cdots & \mathbf{H}_{N,M} \end{bmatrix}}_{\mathbf{H}} \underbrace{\begin{bmatrix} s_1 \\ s_2 \\ \vdots \\ s_{2M-1} \\ s_{2M} \end{bmatrix}}_{\mathbf{s}} + \underbrace{\begin{bmatrix} w_{1,1} \\ -w_{1,2}^* \\ \vdots \\ w_{N,1} \\ -w_{N,2}^* \end{bmatrix}}_{\mathbf{w}}$$

$$\mathbf{H}_{n,m} \square \begin{bmatrix} h_{n,2m-1} & h_{n,2m} \\ -h_{n,2m}^* & h_{n,2m-1}^* \end{bmatrix}, \quad \forall n \text{ and } m$$

$$M = 2, N = 2$$

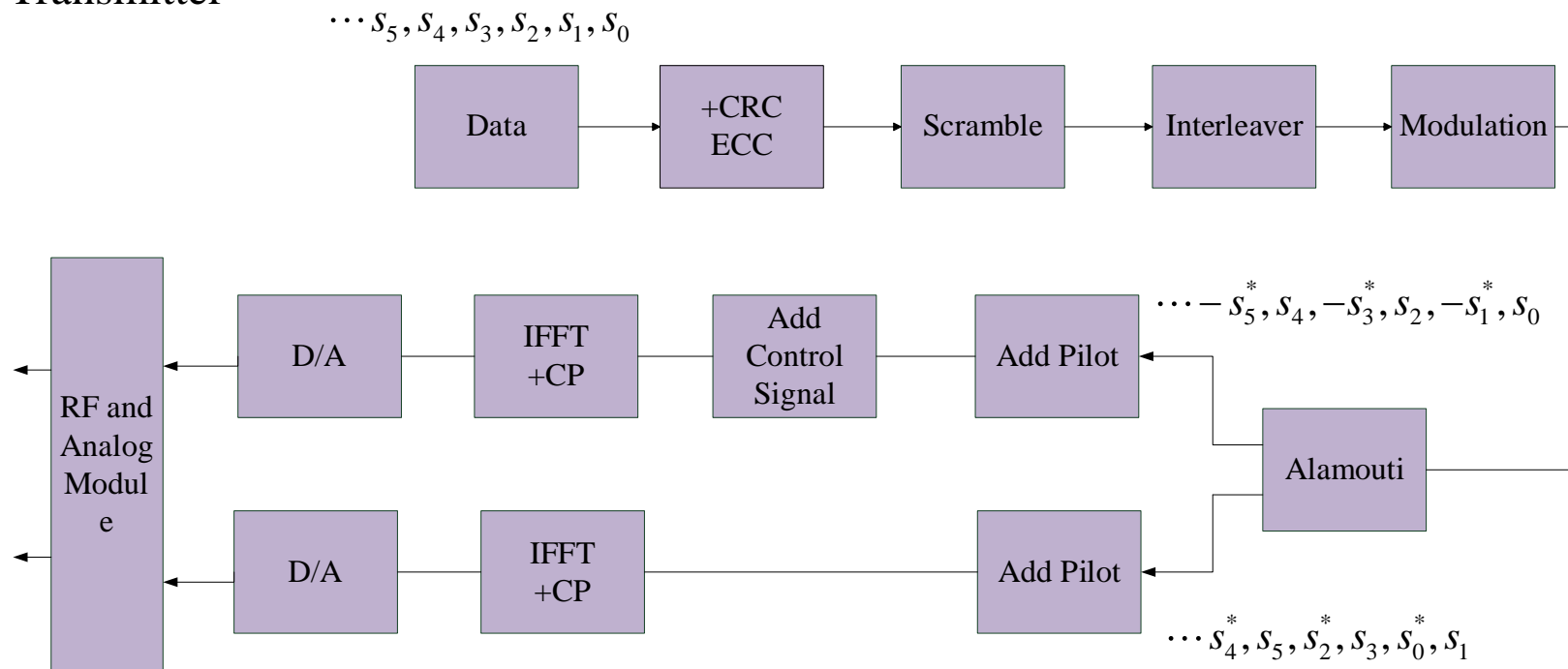
$$\underbrace{\begin{bmatrix} x_{1,1} \\ -x_{1,2}^* \\ x_{2,1} \\ -x_{2,2}^* \end{bmatrix}}_{\mathbf{x}} = \underbrace{\begin{bmatrix} h_{1,1} & h_{1,2} & h_{1,3} & h_{1,4} \\ -h_{1,2}^* & h_{1,1}^* & -h_{1,4}^* & h_{1,3}^* \\ h_{2,1} & h_{2,2} & h_{2,3} & h_{2,4} \\ -h_{2,2}^* & h_{2,1}^* & -h_{2,4}^* & h_{2,3}^* \end{bmatrix}}_{\mathbf{H}} \underbrace{\begin{bmatrix} s_1 \\ s_2 \\ s_3 \\ s_4 \end{bmatrix}}_{\mathbf{s}} + \underbrace{\begin{bmatrix} w_{1,1} \\ -w_{1,2}^* \\ w_{2,1} \\ -w_{2,2}^* \end{bmatrix}}_{\mathbf{w}}$$





Alamouti STBC MIMO

Transmitter



Transmit Time

Antenna 1

Antenna 2

t

s_1

s_2

$t + T_s$

$-s_2^*$

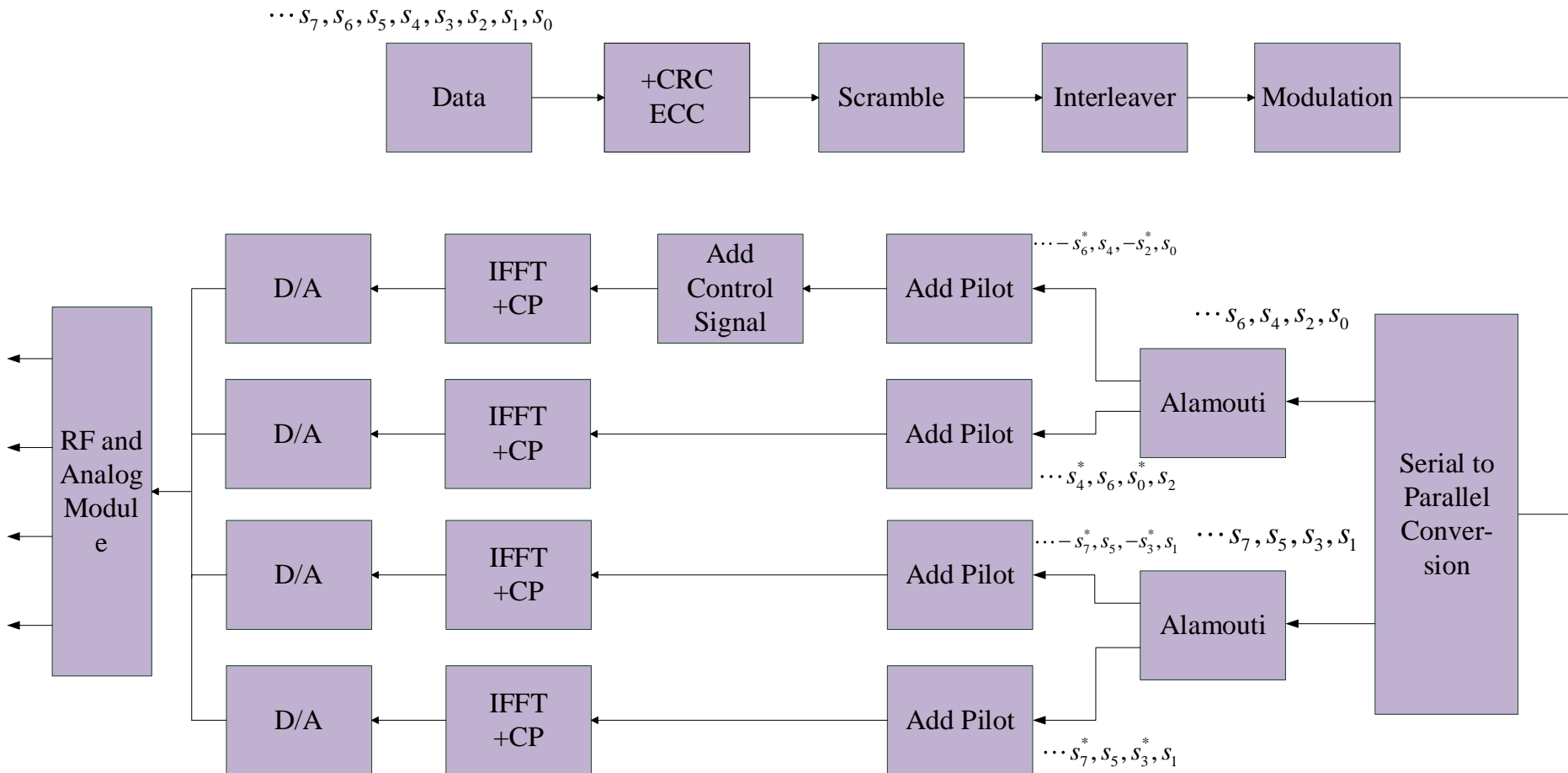
s_1^*





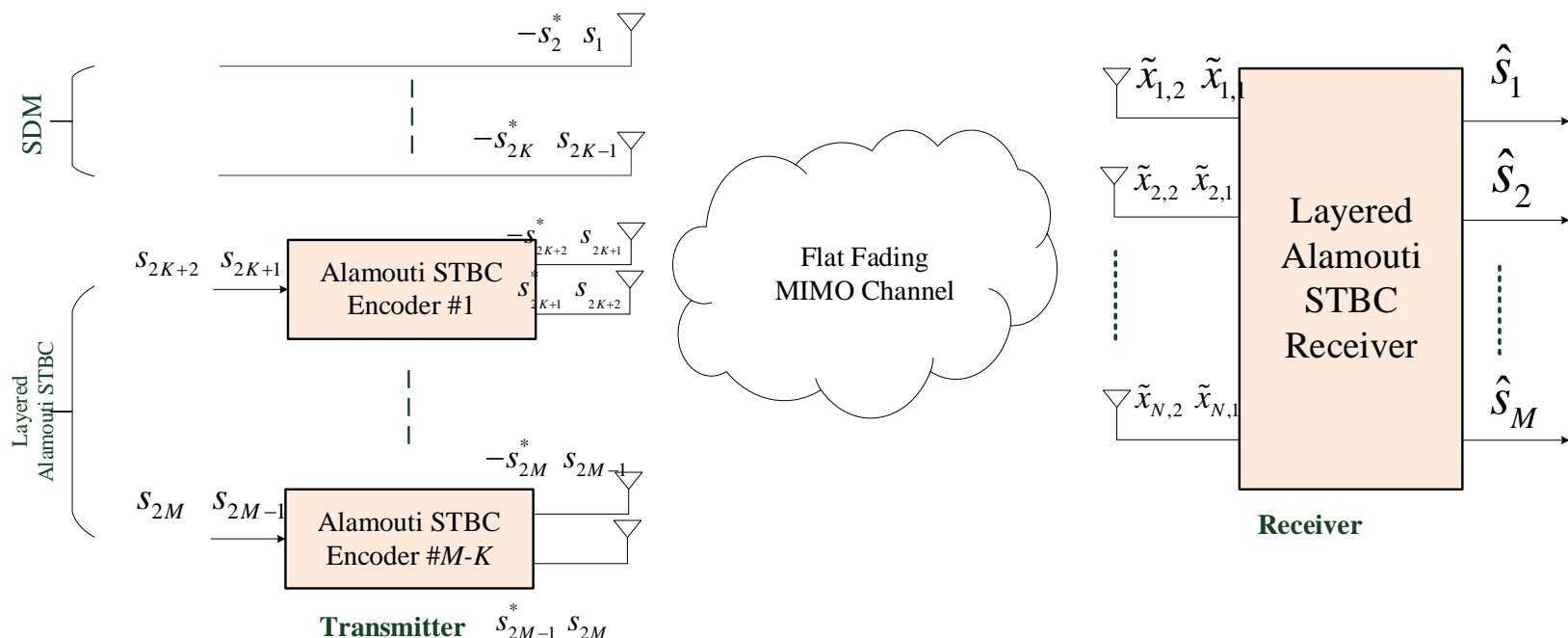
Double Space-Time Transmit Diversity, DSTTD

Transmitter





Hybrid Alamouti STBC MIMO



The hybrid Alamouti STBC MIMO system transmits every $2M$ symbols over two time instants using $2M - K$ transmit antennas

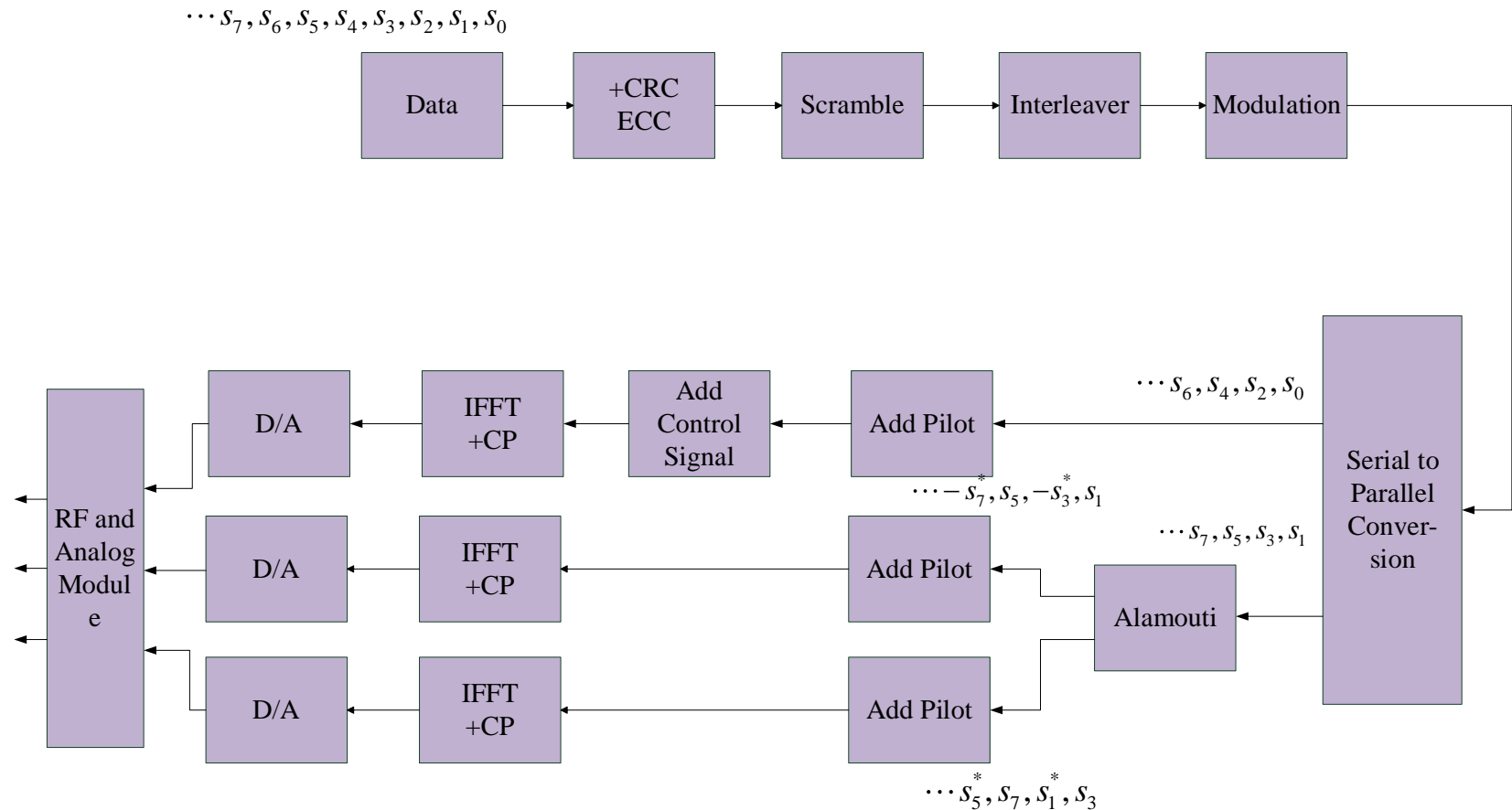
$$\begin{bmatrix} \tilde{x}_{1,1} & \tilde{x}_{1,2} \\ \vdots & \vdots \\ \tilde{x}_{N,1} & \tilde{x}_{N,2} \end{bmatrix} = \begin{bmatrix} h_{1,1} & \cdots & h_{1,2M-K} \\ \vdots & \ddots & \vdots \\ h_{N,1} & \cdots & h_{N,2M-K} \end{bmatrix} \begin{bmatrix} s_1 & -s_2^* \\ \vdots & \vdots \\ \frac{s_{2K-1} - s_{2K}^*}{\mathbf{S}_{K+1}} \\ \vdots \\ \mathbf{S}_M \end{bmatrix} + \tilde{\mathbf{W}}, \quad \mathbf{S}_m \square \begin{bmatrix} s_{2m-1} & -s_{2m}^* \\ s_{2m} & s_{2m-1}^* \end{bmatrix}$$





Hybrid Alamouti STBC MIMO

Transmitter





Hybrid Alamouti STBC MIMO

Convert to linear model

$$\underbrace{\begin{bmatrix} \tilde{x}_{1,1} \\ -\tilde{x}_{1,2}^* \\ \vdots \\ \tilde{x}_{N,1} \\ -\tilde{x}_{N,2}^* \end{bmatrix}}_{\tilde{\mathbf{x}}} = \tilde{\mathbf{H}} \underbrace{\begin{bmatrix} s_1 \\ \vdots \\ \frac{s_{2K}}{\mathbf{S}_{2K+1}} \\ \vdots \\ \mathbf{S}_{2M} \end{bmatrix}}_s + \underbrace{\begin{bmatrix} \tilde{w}_{1,1} \\ \tilde{w}_{1,2}^* \\ \vdots \\ \tilde{w}_{N,1} \\ \tilde{w}_{N,2}^* \end{bmatrix}}_{\tilde{\mathbf{w}}}$$

$$\tilde{\mathbf{H}} \triangleq \begin{bmatrix} \mathbf{\Lambda}_{1,1} & \cdots & \mathbf{\Lambda}_{1,K} & \mathbf{H}_{1,K+1} & \cdots & \mathbf{H}_{1,M} \\ \vdots & \ddots & \vdots & \vdots & \ddots & \vdots \\ \mathbf{\Lambda}_{N,1} & \cdots & \mathbf{\Lambda}_{N,K} & \mathbf{H}_{N,K+1} & \cdots & \mathbf{H}_{N,M} \end{bmatrix}$$

$$\mathbf{\Lambda}_{n,k} \triangleq \begin{bmatrix} h_{n,k} & 0 \\ 0 & h_{n,k}^* \end{bmatrix} \quad \mathbf{H}_{n,m} \triangleq \begin{bmatrix} h_{n,m} & h_{n,2m-1} \\ -h_{n,2m-1}^* & h_{n,m}^* \end{bmatrix}, \quad \forall n \text{ and } m$$

$$N = 2, M = 2, K = 1$$

$$\begin{bmatrix} x_{1,1} \\ -x_{1,2}^* \\ x_{2,1} \\ -x_{2,2}^* \end{bmatrix} = \begin{bmatrix} h_{1,1} & 0 & h_{1,2} & h_{1,3} \\ 0 & h_{1,1}^* & -h_{1,3}^* & h_{1,2}^* \\ h_{2,1} & 0 & h_{2,2} & h_{2,3} \\ 0 & h_{2,1}^* & -h_{2,3}^* & h_{2,2}^* \end{bmatrix} \begin{bmatrix} s_1 \\ s_2 \\ s_3 \\ s_4 \end{bmatrix} + \mathbf{w}$$





Detection for Layered Alamouti STBC Signals

Base on the linear model, the maximum likelihood (ML) detection of \mathbf{s} from observation \mathbf{x} is

$$\hat{\mathbf{s}}_{ML} = \arg \min_{\mathbf{s} \in \Omega^{2M}} \|\mathbf{x} - \mathbf{H}\mathbf{s}\|^2, \text{ where } \Omega \text{ denotes the set of constellation points for each symbol } s_m.$$

With the QRD of $\mathbf{H} = \mathbf{QR}$, the ML detection becomes $\hat{\mathbf{s}}_{ML} = \arg \min_{\mathbf{s} \in \Omega^{2M}} \|\mathbf{Q}^H \mathbf{x} - \mathbf{Rs}\|^2$.

Corollary 1: Let \mathbf{U} and \mathbf{V} be $2n \times 2m$ and $2m \times 2k$ matrices, respectively, comprised of Alamouti sub-blocks.

The product \mathbf{UV} is comprised of Alamouti sub-blocks.

Lemma 1: The QRD of the $\mathbf{H} = \mathbf{QR}$ produces matrices with Alamouti sub-blocks, i.e.,

$$\mathbf{Q} \triangleq \begin{bmatrix} \mathbf{Q}_{1,1} & \cdots & \mathbf{Q}_{1,M} \\ \vdots & \ddots & \vdots \\ \mathbf{Q}_{N,1} & \cdots & \mathbf{Q}_{N,M} \end{bmatrix} \text{ and } \mathbf{R} \triangleq \begin{bmatrix} \mathbf{R}_{1,1} & \cdots & \mathbf{R}_{1,M} \\ & \ddots & \vdots \\ \mathbf{0} & & \mathbf{R}_{M,M} \end{bmatrix},$$

with Alamouti sub-blocks

$$\mathbf{Q}_{n,m} \triangleq \begin{bmatrix} q_{n,2m-1} & q_{n,2m} \\ -q_{n,2m}^* & q_{n,2m-1}^* \end{bmatrix} \text{ and } \mathbf{R}_{n,m} \triangleq \begin{bmatrix} r_{n,2m-1} & r_{n,2m} \\ -r_{n,2m}^* & r_{n,2m-1}^* \end{bmatrix}.$$





BCGR (Block-wise Complex Givens Rotation) (1/2)

Consider an Alamouti block

$$\mathbf{A} \triangleq \begin{bmatrix} a_1 & -a_2^* \\ a_2 & a_1^* \end{bmatrix} = \begin{bmatrix} |a_1| e^{j\phi_{a1}} & -|a_2| e^{-j\phi_{a2}} \\ |a_2| e^{j\phi_{a2}} & |a_1| e^{-j\phi_{a1}} \end{bmatrix}.$$

We can diagonalize \mathbf{A} by

$$\underbrace{\sqrt{|a_1|^2 + |a_2|^2}}_{\sqrt{\alpha}} \mathbf{I}_2 = \underbrace{\begin{bmatrix} 1 & 0 \\ 0 & e^{j(\phi_{a1} + \phi_{a2})} \end{bmatrix} \begin{bmatrix} \cos \phi_{a_1 a_2} & \sin \phi_{a_1 a_2} \\ -\sin \phi_{a_1 a_2} & \cos \phi_{a_1 a_2} \end{bmatrix} \begin{bmatrix} e^{-j\phi_{a1}} & 0 \\ 0 & e^{-j\phi_{a2}} \end{bmatrix}}_{\mathbf{T}_a} \mathbf{A},$$

where $\phi_{a_1 a_2} = \tan^{-1}(|a_2|/|a_1|)$.

Compared with TACR, it is rotated by two more angles ϕ_{a1} and ϕ_{a2} , respectively

Similarly, a different Alamouti matrix

$$\mathbf{B} \triangleq \begin{bmatrix} b_1 & -b_2^* \\ b_2 & b_1^* \end{bmatrix} = \begin{bmatrix} |b_1| e^{j\phi_{b1}} & -|b_2| e^{-j\phi_{b2}} \\ |b_2| e^{j\phi_{b2}} & |b_1| e^{-j\phi_{b1}} \end{bmatrix}$$

can also be diagonalized by

$$\underbrace{\sqrt{|b_1|^2 + |b_2|^2}}_{\sqrt{\beta}} \mathbf{I}_2 = \underbrace{\begin{bmatrix} \cos \phi_{b_1 b_2} e^{-j\phi_{b1}} & \sin \phi_{b_1 b_2} e^{-j\phi_{b2}} \\ -\sin \phi_{b_1 b_2} e^{j\phi_{b2}} & \cos \phi_{b_1 b_2} e^{j\phi_{b1}} \end{bmatrix}}_{\mathbf{T}_b} \mathbf{B},$$

where $\phi_{b_1 b_2} = \tan^{-1}(|b_2|/|b_1|)$.



BCGR (Block-wise Complex Givens Rotation) (2/2)

Applying to a matrix with Alamouti sub-blocks **A**, **B**, **C**, and **D**,

we have $\begin{bmatrix} \sqrt{\alpha}\mathbf{I}_2 & \mathbf{C}^{(1)} \\ \sqrt{\beta}\mathbf{I}_2 & \mathbf{D}^{(1)} \end{bmatrix} = \begin{bmatrix} \mathbf{T}_a & 0 \\ 0 & \mathbf{T}_b \end{bmatrix} \begin{bmatrix} \mathbf{A} & \mathbf{C} \\ \mathbf{B} & \mathbf{D} \end{bmatrix}$, where **C** and **D** are changed to Alamouti blocks **C**⁽¹⁾ and **D**⁽¹⁾, respectively.

Next, applying the rotation with $\phi_{ab} = \tan^{-1}(|\beta|/|\alpha|)$ to the matrix on the left-hand-side,

we achieve
$$\begin{bmatrix} \sqrt{\alpha+\beta}\mathbf{I}_2 & \mathbf{C}^{(2)} \\ 0 & \mathbf{D}^{(2)} \end{bmatrix} = \underbrace{\begin{bmatrix} \cos\phi_{ab} & 0 & \sin\phi_{ab} & 0 \\ 0 & \cos\phi_{ab} & 0 & \sin\phi_{ab} \\ -\sin\phi_{ab} & 0 & \cos\phi_{ab} & 0 \\ 0 & -\sin\phi_{ab} & 0 & \cos\phi_{ab} \end{bmatrix}}_{\mathbf{T}_{ab}} \begin{bmatrix} \sqrt{\alpha}\mathbf{I}_2 & \mathbf{C}^{(1)} \\ \sqrt{\beta}\mathbf{I}_2 & \mathbf{D}^{(1)} \end{bmatrix},$$

where **C**⁽¹⁾ and **D**⁽¹⁾ are rotated to Alamouti blocks **C**⁽²⁾ and **D**⁽²⁾, respectively.



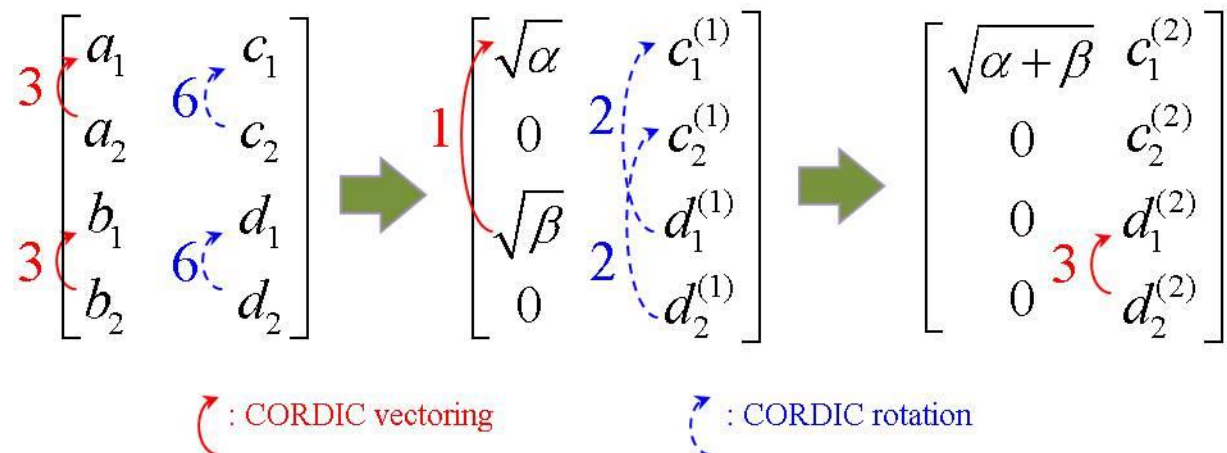


Procedure of BCGR Based QRD

BCGR performs in the vectoring in the vetoring and rotation modes to process a 4×4 matrix with Alamouti sub-blocks.

Only the numbers of CORDIC vectoring and rotation operations are given.

Refer to Table I for the exact angles associated with CORDIC vectoring and rotation operations.

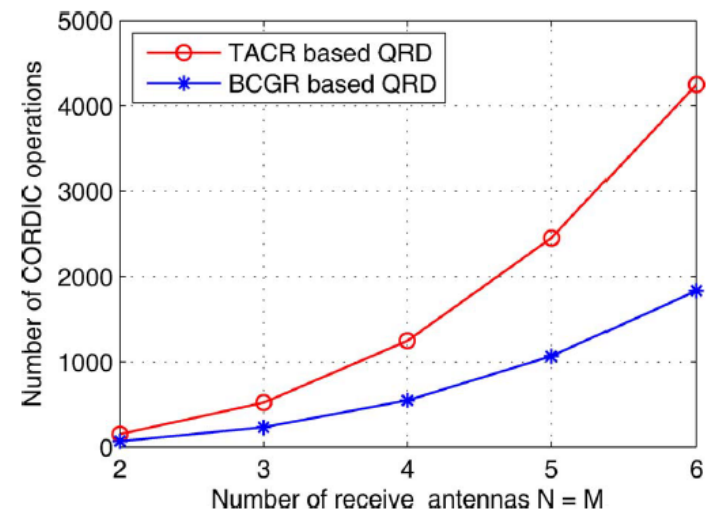




Complexity Comparison of the TACR and BCGR Based QRDs

Complexity comparison of the TACR and BCGR based QRDs of an $2M \times 2M$ matrix \mathbf{H} with Alamouti sub-blocks

	TACR based QRD	BCGR based QRD
Number of CORDIC vectoring operations to compute \mathbf{R}	$4M^2$	$2M^2 + M$
Number of CORDIC rotation operations to compute \mathbf{R}	$8M^3 - 4M^2$	$(10/3)M^3 - 2M^2 - (4/3)M$
Number of CORDIC rotation operations to compute \mathbf{Q}	$12M^3 - 2M^2$	$5M^3 + M^2$
Total number of CORDIC operations to compute \mathbf{Q} and \mathbf{R}	$20M^3 - 2M^2$	$(25/3)M^3 + M^2 - (1/3)M$



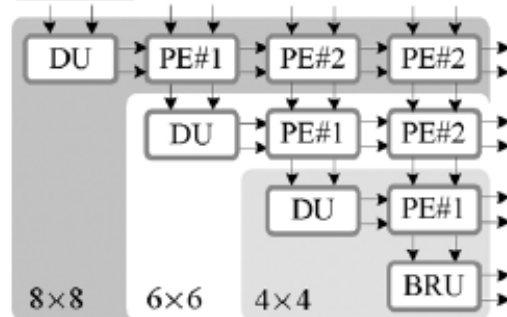


BCGR-TSA Architecture (1/2)

BCGR-TSA architecture for the QRD of $8 \times 8 \mathbf{H}$ with

Alamouti sub-blocks

$$\begin{matrix}
 & & & \vdots & \vdots & 1 & 0 \\
 & & & 0 & 0 & 0 & 0 \\
 & & 0 & 0 & 1 & 0 & 0 \\
 0 & 0 & 0 & 0 & 0 & 0 & 0 \\
 0 & 0 & 1 & 0 & 0 & 0 & \boxed{h_{4,7} - h_{4,8}} \\
 0 & 0 & 0 & 0 & h_{3,7} - h_{3,8} & h_{4,5} - h_{4,6} \\
 1 & 0 & h_{2,7} - h_{2,8} & \boxed{h_{3,5} - h_{3,6}} & h_{4,3} - h_{4,4} \\
 h_{1,7} - h_{1,8} & h_{2,5} - h_{2,6} & h_{3,3} - h_{3,4} & h_{4,1} - h_{4,2} \\
 h_{1,5} - h_{1,6} & \boxed{h_{2,3} - h_{2,4}} & h_{3,1} - h_{3,2} \\
 h_{1,3} - h_{1,4} & h_{2,1} - h_{2,2} \\
 h_{1,1} - h_{1,2}
 \end{matrix}$$

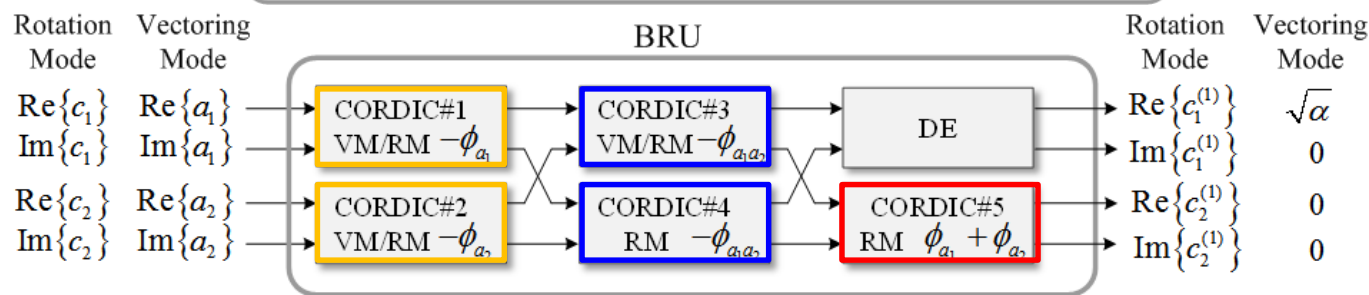
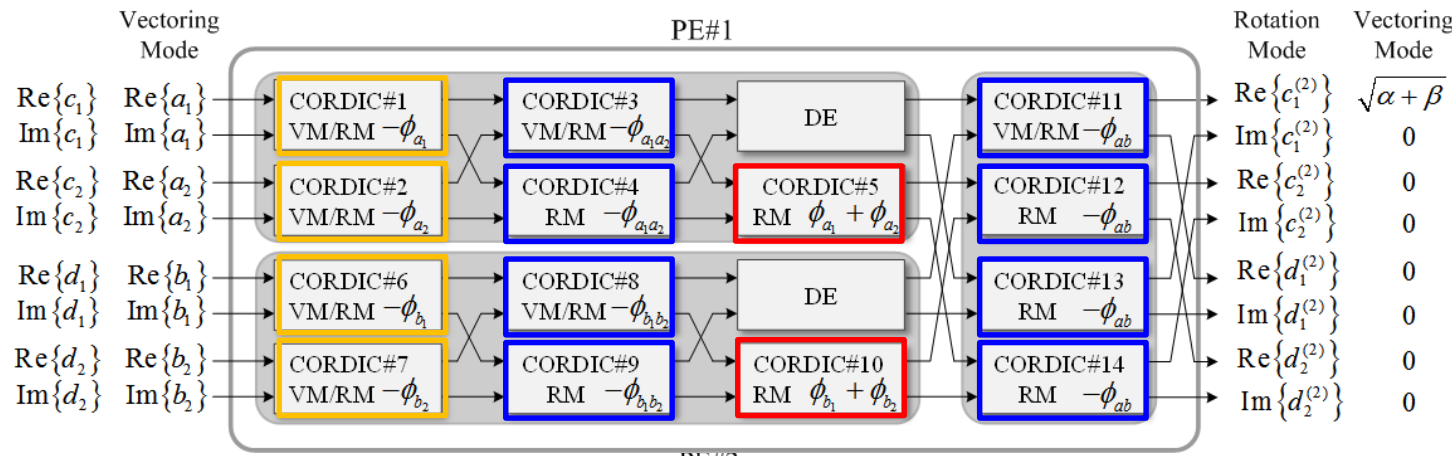


$$\begin{bmatrix}
 h_{1,1} & h_{1,2} & h_{1,3} & h_{1,4} & h_{1,5} & h_{1,6} & h_{1,7} & h_{1,8} \\
 -h_{1,2}^* & h_{1,1}^* & -h_{1,4}^* & h_{1,3}^* & -h_{1,6}^* & h_{1,5}^* & -h_{1,8}^* & h_{1,7}^* \\
 \hline
 h_{2,1} & h_{2,2} & h_{2,3} & h_{2,4} & h_{2,5} & h_{2,6} & h_{2,7} & h_{2,8} \\
 -h_{2,2}^* & h_{2,1}^* & -h_{2,4}^* & h_{2,3}^* & -h_{2,6}^* & h_{2,5}^* & -h_{2,8}^* & h_{2,7}^* \\
 \hline
 h_{3,1} & h_{3,2} & h_{3,3} & h_{3,4} & h_{3,5} & h_{3,6} & h_{3,7} & h_{3,8} \\
 -h_{3,2}^* & h_{3,1}^* & -h_{3,4}^* & h_{3,3}^* & -h_{3,6}^* & h_{3,5}^* & -h_{3,8}^* & h_{3,7}^* \\
 \hline
 h_{4,1} & h_{4,2} & h_{4,3} & h_{4,4} & h_{4,5} & h_{4,6} & h_{4,7} & h_{4,8} \\
 -h_{4,2}^* & h_{4,1}^* & -h_{4,4}^* & h_{4,3}^* & -h_{4,6}^* & h_{4,5}^* & -h_{4,8}^* & h_{4,7}^*
 \end{bmatrix}$$

$$\begin{array}{ccccccccc}
 \dots & q_{1,7} & q_{1,5} & q_{1,3} & q_{1,1} & r_{1,7} & r_{1,5} & r_{1,3} & r_{1,1} \\
 \dots & -q_{1,8}^* & -q_{1,6}^* & -q_{1,4}^* & -q_{1,2}^* & -r_{1,8}^* & -r_{1,6}^* & -r_{1,4}^* & 0 \\
 \dots & q_{2,7} & q_{2,5} & q_{2,3} & q_{2,1} & r_{2,7} & r_{2,5} & r_{2,3} & 0 \\
 \dots & -q_{2,8}^* & -q_{2,6}^* & -q_{2,4}^* & -q_{2,2}^* & -r_{2,8}^* & -r_{2,6}^* & 0 & 0 \\
 \dots & q_{3,7} & q_{3,5} & q_{3,3} & q_{3,1} & r_{3,7} & r_{3,5} & 0 & 0 \\
 \dots & -q_{3,8}^* & -q_{3,6}^* & -q_{3,4}^* & -q_{3,2}^* & -r_{3,8}^* & 0 & 0 & 0 \\
 \dots & q_{4,7} & q_{4,5} & q_{4,3} & q_{4,1}^* & r_{4,7} & 0 & 0 & 0 \\
 \dots & -q_{4,8}^* & -q_{4,6}^* & -q_{4,4}^* & -q_{4,2}^* & 0 & 0 & 0 & 0
 \end{array}$$



BCGR-TSA Architecture (2/2)



VM下
同時提供look-up-table free 及
傳統的角度表示法
RM下以look-up-table free
的方向資訊做旋轉運算
look-up-table free
conventional





Architectural Comparisons of the TACR-TSA and BCGR-TSA

Architectural comparision of the TACR-TSA and BCGR-TSA
to compute the QRD of a $2M \times 2M$ channel matrix with
Alamouti sub-blocks

	TACR-TSA	BCGR-TSA
Number of CORDIC modules in a PE#1	4	14
Number of PE#1 modules	$2M - 1$	$M - 1$
Number of CORDIC modules in a PE#2	3	9
Number of PE#2 modules	$2M^2 - 3M + 1$	$(1/2)M^2 - (3/2)M + 1$
Number of CORDIC modules in the rotation unit	1	5
Number of rotation unit	1	1
Total number of CORDIC modules in the TSA	$6M^2 - M$	$(9/2)M^2 + (1/2)M$
Latency of a PE (clock cycles)	6	12
Processing cycles (clock cycles)	$4M$	$2M$
Processing Latency (clock cycles)	$28M - 10$	$26M - 16$





Comparisons with Other Architectures

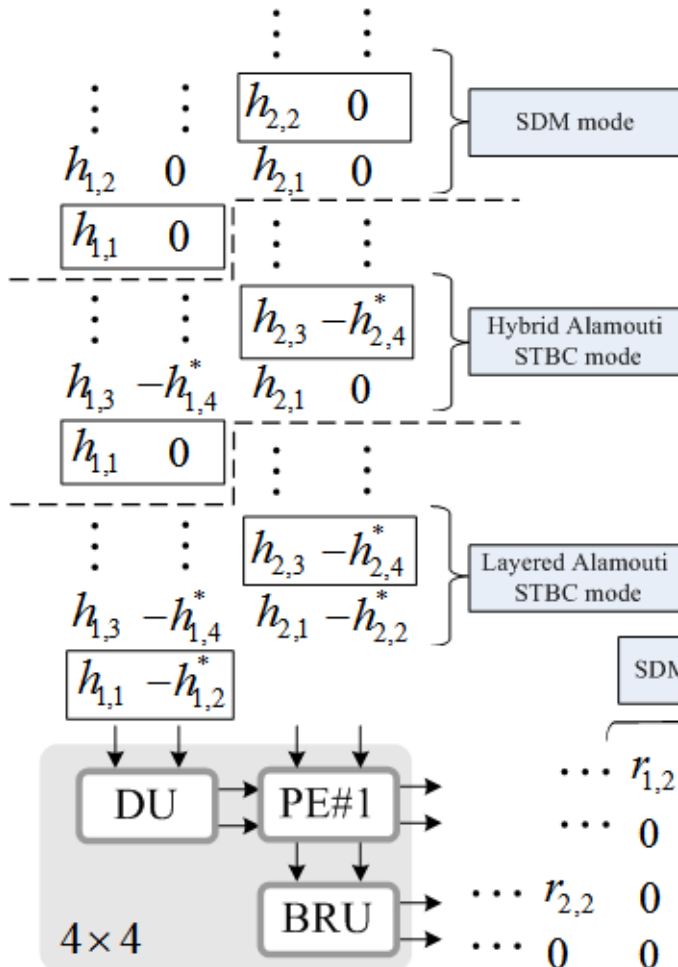
Architecture	[21]	[22]	[23]	[24]	[27]	TACR-TSA[36]	BCGR-TSA (Proposed)		
System	SDM	SDM	SDM	SDM	SDM	SDM	Layered Alamouti STBC		
Antennas (Tx × Rx)	(4 × 4)	(2 × 2)	(4 × 4)	(4 × 4)	(4 × 4)	(4 × 4)	(4 × 2)	(8 × 4)	
Complex/Real (Matrix Size)	Complex (4 × 4)	Real (4 × 4)	Complex (4 × 4)	Complex (8 × 8)					
Algorithm	GR	MGS	GR	GR	GR	GR	GR	GR	
Matrix R or (Q, R)	R	(Q, R)	R	R	R	(Q, R)	(Q, R)	(Q, R)	
CMOS Technology	0.13 μm	0.18 μm	0.18 μm	0.18 μm	0.18 μm	90 nm	90 nm	90 nm	
Frequency (MHz)	270	400	100	120	200	125.4		125.4	
Gate Count	36 K	32.6 K	111 K	134.6 K	103.7 K	132 K	575 K	115 K	471 K
Processing Cycles (clock cycles)	20	35	4	8	8	8	16	4	8
Processing Latency (clock cycles)	20	35	30	92	91	46	102	36	88
Throughput Rate (QRDs/s)	6.75 M	11.4 M	12.5 M	7.5 M	12.5 M	15.68 M	7.84 M	31.35 M	15.68 M





Extension to the Hybrid Alamouti STBC and SDM system

Three modes of the MIMO system with 2 receive antennas



Mode	(N, M, K)	Antenna configuration (Tx \times Rx)	Equivalent channel matrix
Layered Alamouti STBC	$(2, 2, 0)$	4×2	$\begin{bmatrix} \mathbf{H}_{1,1} & \mathbf{H}_{1,2} \\ \mathbf{H}_{2,1} & \mathbf{H}_{2,2} \end{bmatrix}$
Layered Alamouti STBC	$(2, 2, 1)$	3×2	$\begin{bmatrix} \mathbf{\Lambda}_{1,1} & \mathbf{H}_{1,2} \\ \mathbf{\Lambda}_{2,1} & \mathbf{H}_{2,2} \end{bmatrix}$
SDM	$(2, 2, 1)$	2×2	$\begin{bmatrix} \mathbf{\Lambda}_{1,1} & \mathbf{\Lambda}_{1,2} \\ \mathbf{\Lambda}_{2,1} & \mathbf{\Lambda}_{2,2} \end{bmatrix}$

$$\begin{array}{ccc}
 \cdots & r_{1,2} & r_{1,1} \\
 \cdots & 0 & 0 \\
 & \cdots & \cdots \\
 & r_{2,2} & 0 \\
 & \cdots & \cdots \\
 & 0 & 0
 \end{array}
 \quad
 \boxed{
 \begin{array}{cc}
 \cdots & r_{1,3} \\
 \cdots & r_{1,1} \\
 \cdots & -r_{1,4}^* \\
 & 0 \\
 \cdots & r_{2,2} \\
 & 0
 \end{array}
 }
 \quad
 \boxed{
 \begin{array}{cc}
 \cdots & r_{1,3} \\
 \cdots & r_{1,1} \\
 \cdots & -r_{1,4}^* \\
 & 0 \\
 \cdots & r_{2,2} \\
 & 0
 \end{array}
 }$$

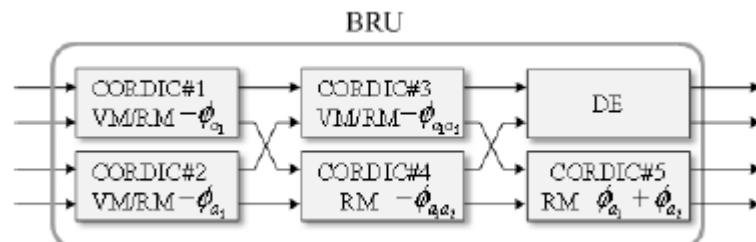
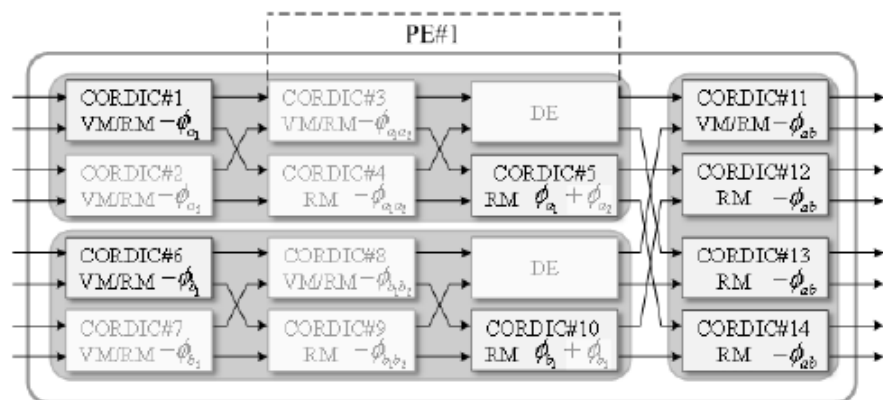




The Architecture Design for the Hybrid Alamouti STBC MIMO System

	Angles obtained or rotated by BCGR	Enabled CORDIC modules in PE#1
angles from vectoring on $\begin{bmatrix} \mathbf{A} \\ \mathbf{B} \end{bmatrix}$ if both \mathbf{A} and \mathbf{B} are diagonal	$\phi_{a_1}, \phi_{b_1}, \phi_{ab}$	1, 6, 11
angles for rotation to $\begin{bmatrix} \mathbf{C} \\ \mathbf{D} \end{bmatrix}$ if both \mathbf{C} and \mathbf{D} are diagonal	$-\phi_{a_1}, -\phi_{b_1}, -2\phi_{ab}$	1, 6, 11, 13
angles for rotation to complex $\begin{bmatrix} \mathbf{C} \\ \mathbf{D} \end{bmatrix}$	$-\phi_{a_1}, \phi_{a_1}, -\phi_{b_1}, \phi_{b_1}, -4\phi_{ab}$	1, 5, 6, 10, 11, 12, 13, 14
angles from vectoring on $\begin{bmatrix} \mathbf{A} \\ \mathbf{B} \end{bmatrix}$ if diagonal \mathbf{A} has positive entries and \mathbf{B} is diagonal	ϕ_{b_1}, ϕ_{ab}	6, 11
angles for rotation to $\begin{bmatrix} \mathbf{C} \\ \mathbf{D} \end{bmatrix}$ if both \mathbf{C} and \mathbf{D} are diagonal	$-\phi_{b_1}, -2\phi_{ab}$	6, 11, 13
angles for rotation to complex $\begin{bmatrix} \mathbf{C} \\ \mathbf{D} \end{bmatrix}$	$-\phi_{b_1}, \phi_{b_1}, -4\phi_{ab}$	6, 10, 11, 12, 13, 14

hybrid Alamouti STBC

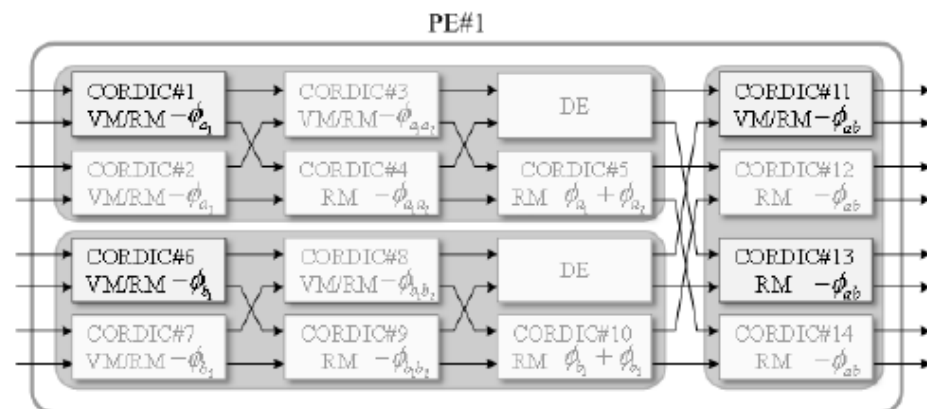




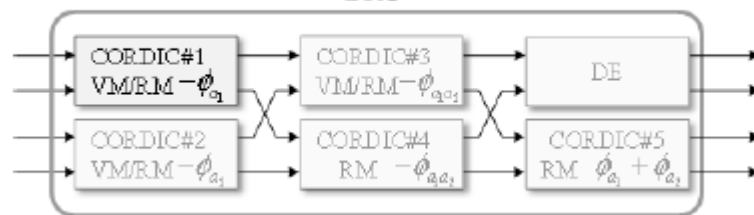
The Architecture Design for the SDM MIMO System

	Angles obtained or rotated by BCGR	Enabled CORDIC modules in PE#1
angles from vectoring on $\begin{bmatrix} \mathbf{A} \\ \mathbf{B} \end{bmatrix}$ if both \mathbf{A} and \mathbf{B} are diagonal	$\phi_{a_1}, \phi_{b_1}, \phi_{ab}$	1, 6, 11
angles for rotation to $\begin{bmatrix} \mathbf{C} \\ \mathbf{D} \end{bmatrix}$ if both \mathbf{C} and \mathbf{D} are diagonal	$-\phi_{a_1}, -\phi_{b_1}, -2\phi_{ab}$	1, 6, 11, 13
angles for rotation to complex $\begin{bmatrix} \mathbf{C} \\ \mathbf{D} \end{bmatrix}$	$-\phi_{a_1}, \phi_{a_1}, -\phi_{b_1}, \phi_{b_1}, -4\phi_{ab}$	1, 5, 6, 10, 11, 12, 13, 14
angles from vectoring on $\begin{bmatrix} \mathbf{A} \\ \mathbf{B} \end{bmatrix}$ if diagonal \mathbf{A} has positive entries and \mathbf{B} is diagonal	ϕ_{b_1}, ϕ_{ab}	6, 11
angles for rotation to $\begin{bmatrix} \mathbf{C} \\ \mathbf{D} \end{bmatrix}$ if both \mathbf{C} and \mathbf{D} are diagonal	$-\phi_{b_1}, -2\phi_{ab}$	6, 11, 13
angles for rotation to complex $\begin{bmatrix} \mathbf{C} \\ \mathbf{D} \end{bmatrix}$	$-\phi_{b_1}, \phi_{b_1}, -4\phi_{ab}$	6, 10, 11, 12, 13, 14

SDM



BRU





The Enable CORDIC Modules for the Architecture in PE#1

Mode	Enable CORDIC modules in PE#1		Enable CORDIC modules in BRU		Processing Latency	Processing Cycles
	vectoring	rotation	vectoring	rotation		
Layered Alamouti STBC	1, 2, 5, 6, 7, 10, 11	1, 2, 3, 4, 5, 6, 7, 8, 9, 10, 11, 12, 13, 14	1, 2, 3	1, 2, 3, 4, 5	36	4
Hybrid Alamouti STBC	1, 6, 11	1, 5, 6, 10, 11, 12, 13, 14	1, 2, 3	1, 2, 3, 4, 5	24	4
SDM	1, 6, 11	1, 6, 11, 13	1	1	18	4





Comparisons with Other Architectures

Items	TACR-TSA	BCGR-TSA	BCGR-TSA for the 3-mode	TACR-TSA	BCGR-TSA
Algorithm	GR (CORDIC)	GR (CORDIC)	GR (CORDIC)	GR (CORDIC)	GR (CORDIC)
System (Tx-Rx)	SDM (4x4)	DSTTD (4x2)	MULTIMODE	SDM (8x8)	DSTTD (8x4)
Architecture	TSA	TSA	TSA	TSA	TSA
Complex/Real Matrix (N*N)	Complex 4*4	Complex 4*4	Complex 4*4	Complex 8*8	Complex 8*8
Wordlengths	16	16	16	16	16
Iterations	9	9	9	9	9
Technology	ASIC 90 nm	ASIC 90 nm	ASIC 90 nm	ASIC 90 nm	ASIC 90 nm
Frequency (MHz)	125.4	125.4	125.4	125.4M	125.4
Gate Count	132K	115K	119K	575K	471K
Processing Cycles (clock cycles)	8	4	4	16	8
Processing Latency (clock cycles)	46	36	36/24/18 (DSTTD/Hybrid Alamouti STBC/SDM)	102	88
Power Consumption (mW)	19 at 0.9V	20 at 0.9V	20/16/3 at 0.9V (DSTTD/Hybrid Alamouti STBC/SDM)	50 at 0.9V	78 at 0.9V
Energy consumed per QRD (nJ)	1.21	0.64	0.64/0.51/0.10 (DSTTD/Hybrid Alamouti STBC/SDM)	6.40	4.99



Other Applications of the CORDIC Operations



- Singular Value Decomposition of Matrices
(MIMO precoding techniques)
- Compute the angle of a complex value
(frequency offset estimation)
- Rotate a complex number by an angle
(frequency compensation)
- ...





Part III :

Precoding Techniques

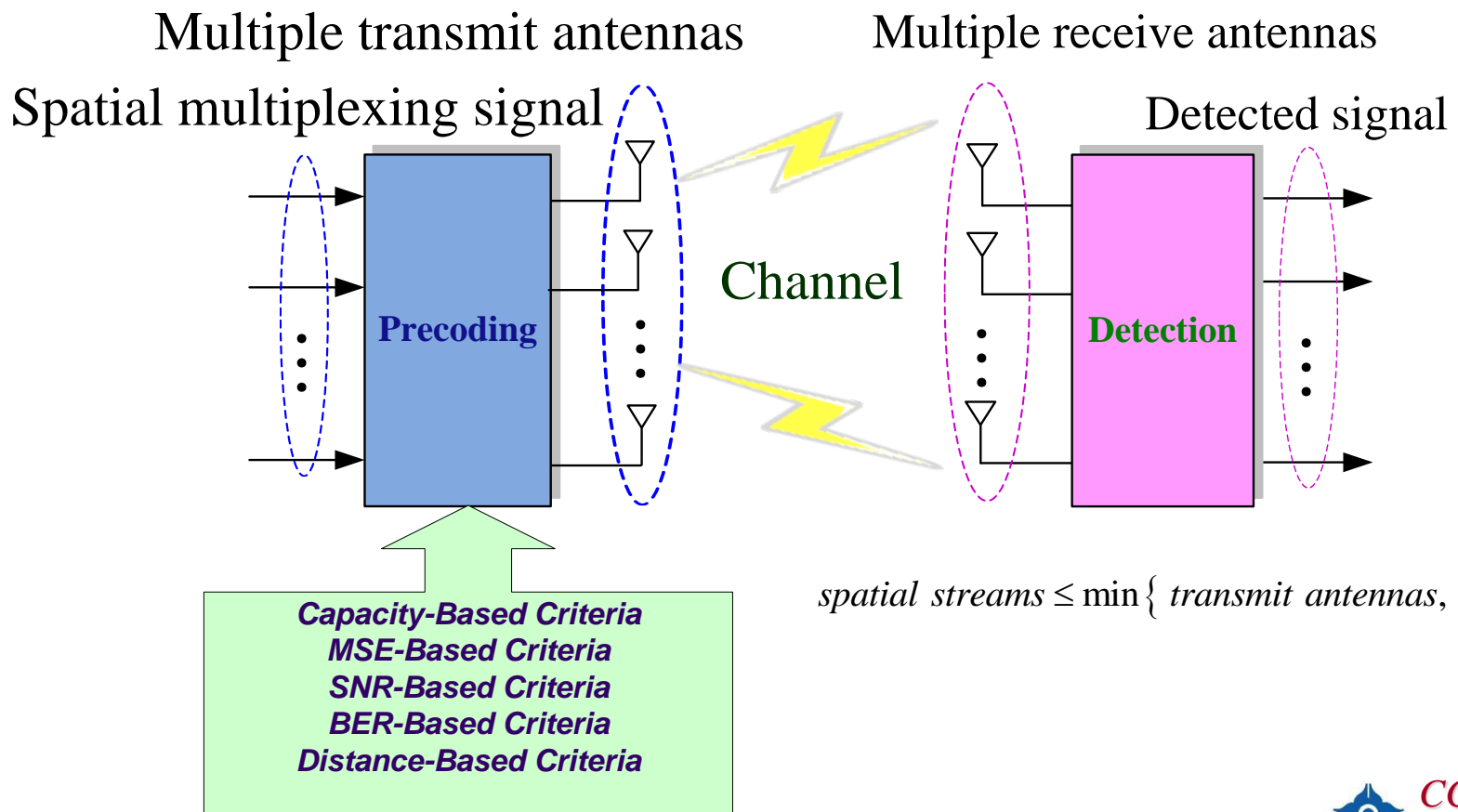
- Precoding Fundamentals
- Compressed Beamforming Weight Precoding
- Codebook Based Precoding





Precoding MIMO System (1/3)

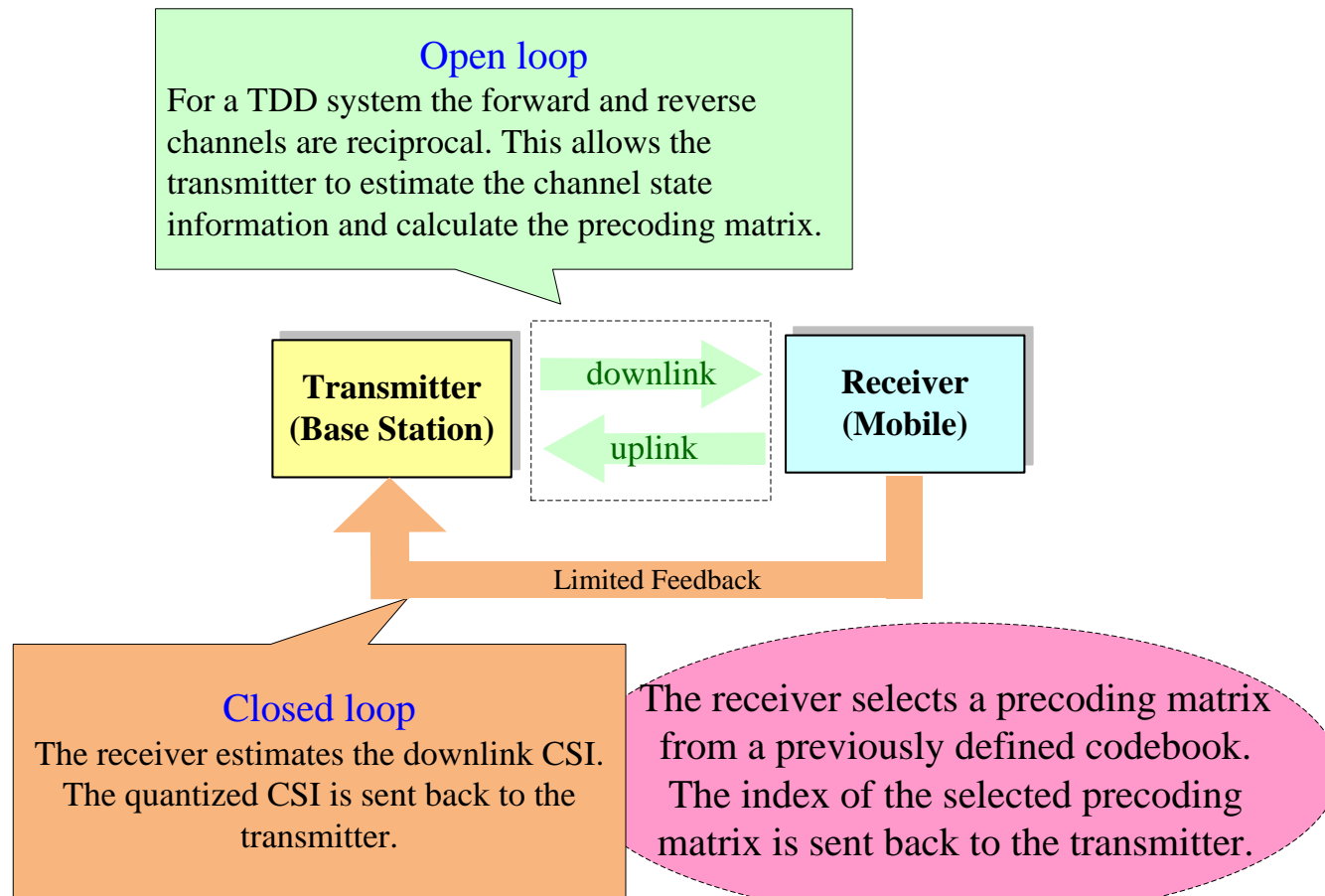
Precoding is a processing technique that exploits CSIT by operating on the signal before transmission to improve the performance of the system. In designing the precoder, various performance criteria have been used.





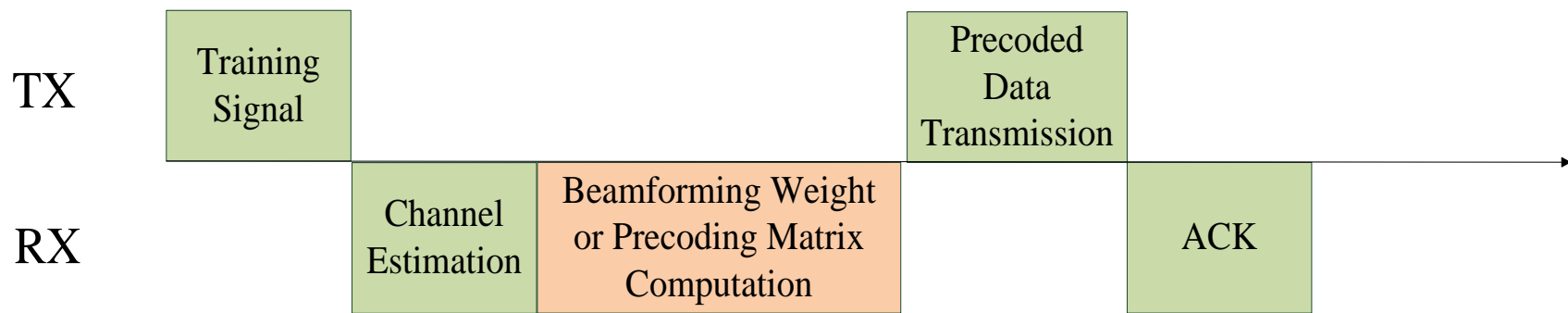
Precoding MIMO System (2/3)

The availability of CSI at the transmitter (CSIT) is possible via feedback or the reciprocal principle when time division duplex (TDD) is used.





Precoding MIMO System (3/3)



Procedure for the precoding MIMO system

**Precoding with at least two spatial streams of signals
or**

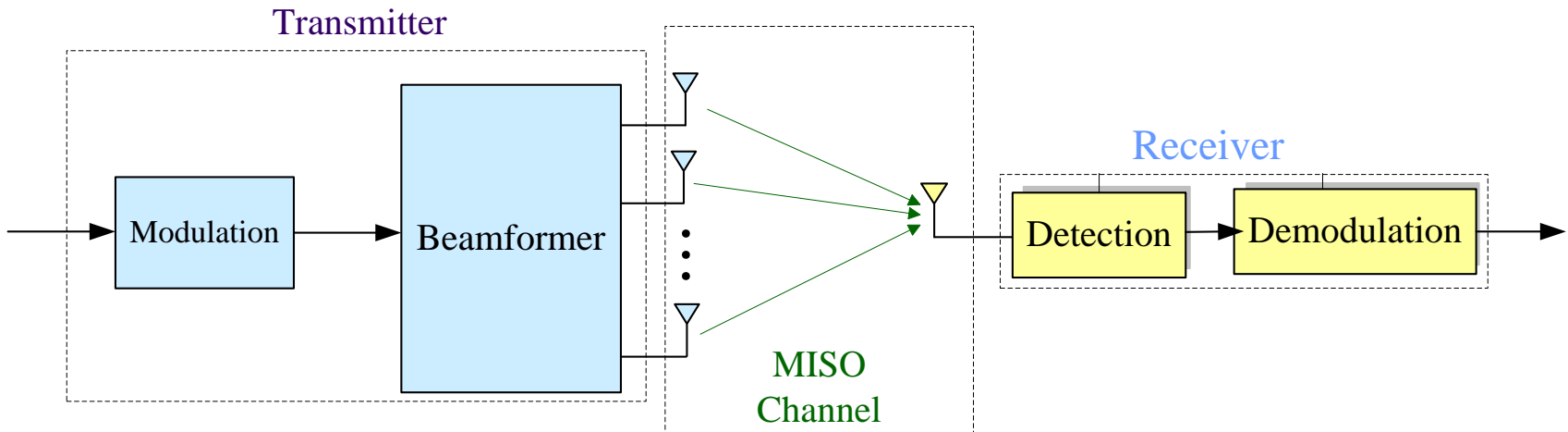
Beamforming with one spatial stream of signal





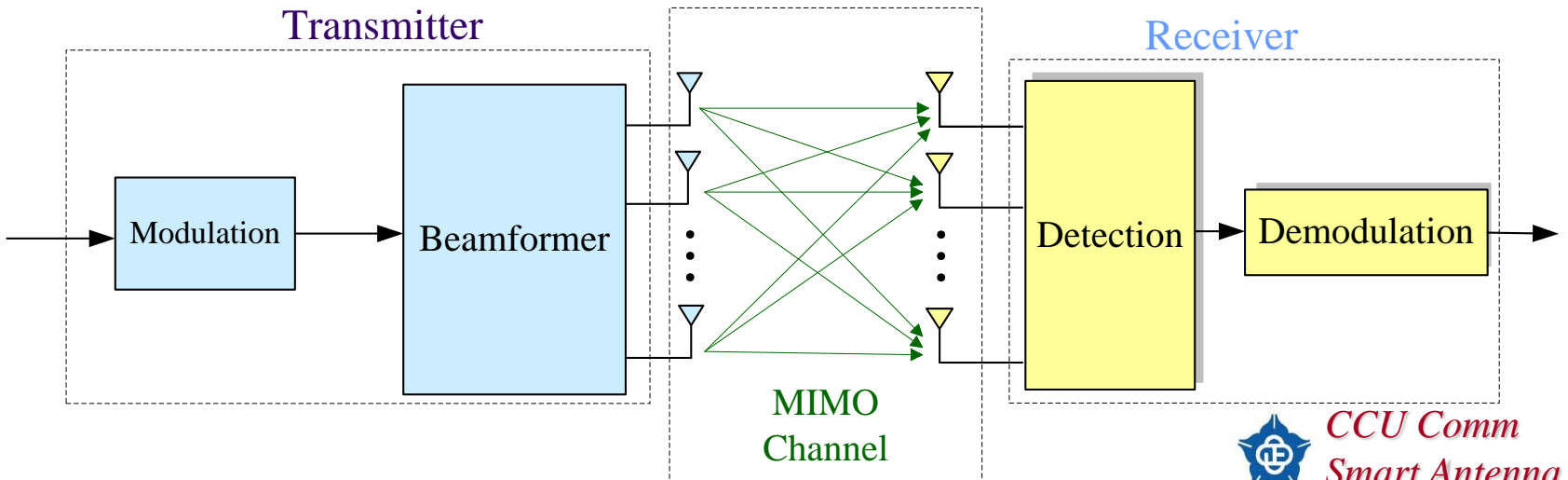
Transmit Beamforming with One Spatial Stream

Transmit beamforming with one receive antenna

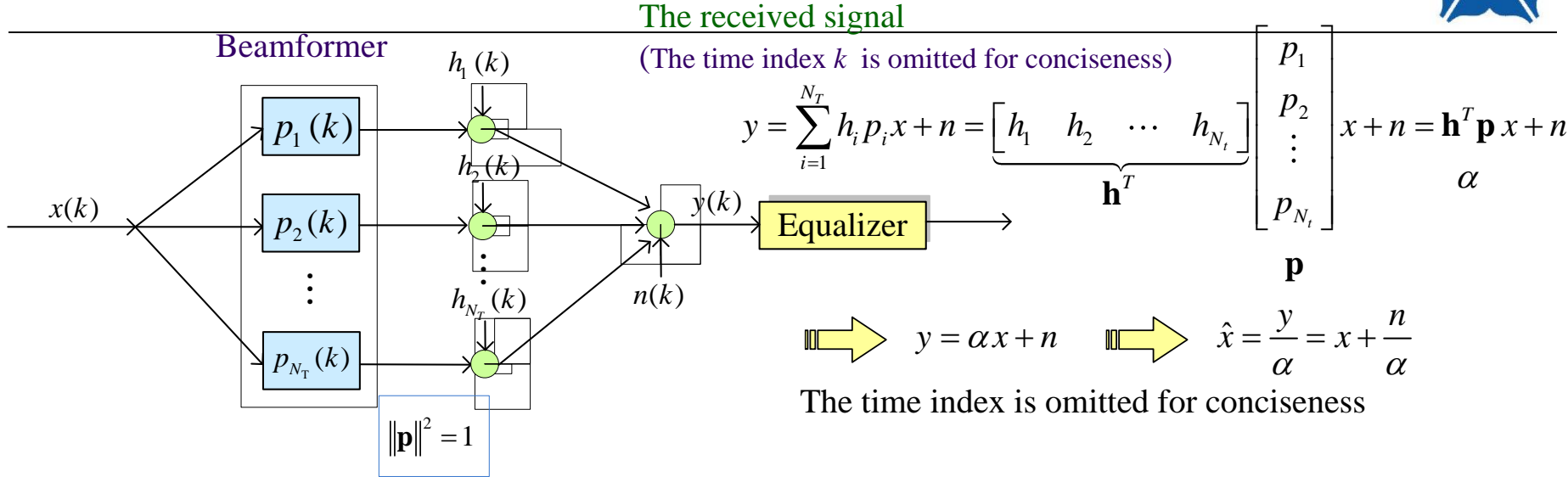


One spatial stream

Transmit beamforming with multiple receive antennas



Transmit Beamforming with One Receive Antenna



The instantaneous SNR at the equalizer output is $\gamma = \frac{\mathbb{E}\{|x|^2\}}{\mathbb{E}\{|n|^2\}} |\alpha|^2 = \frac{E_s}{N_0} |\mathbf{h}^T \mathbf{p}|^2$.

The optimal beamforming vector that maximizes the instantaneous SNR is expressed as

$$\arg \max_{\mathbf{p}} |\mathbf{h}^T \mathbf{p}|^2$$

s.t. $\|\mathbf{p}\|^2 = 1$

The Cauchy-Schwarz inequality $|\mathbf{h}^T \mathbf{p}|^2 \leq \|\mathbf{h}\|^2 \|\mathbf{p}\|^2 \leq \|\mathbf{h}\|^2 \Rightarrow \mathbf{p} = \frac{\mathbf{h}^*}{\|\mathbf{h}\|}$

For the optimal beamformer, the instantaneous SNR at the equalizer output is $\gamma = \frac{E_s}{N_0} \|\mathbf{h}\|^2 \sim \chi^2(2N_t)$.

\Rightarrow The instantaneous BER \Rightarrow The theoretical average BER

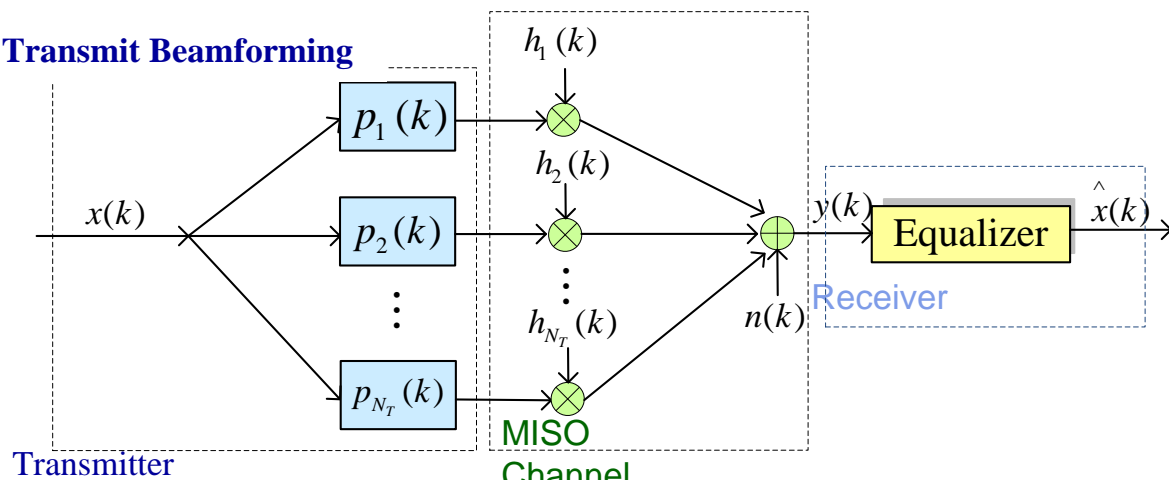


Comparisons Between

Transmit Beamforming and Receive MRC



Transmit Beamforming



Signal model

$$y = \sum_{i=1}^{N_t} h_i p_i x + n = \mathbf{h}^T \mathbf{p} x + n$$

$$\alpha$$

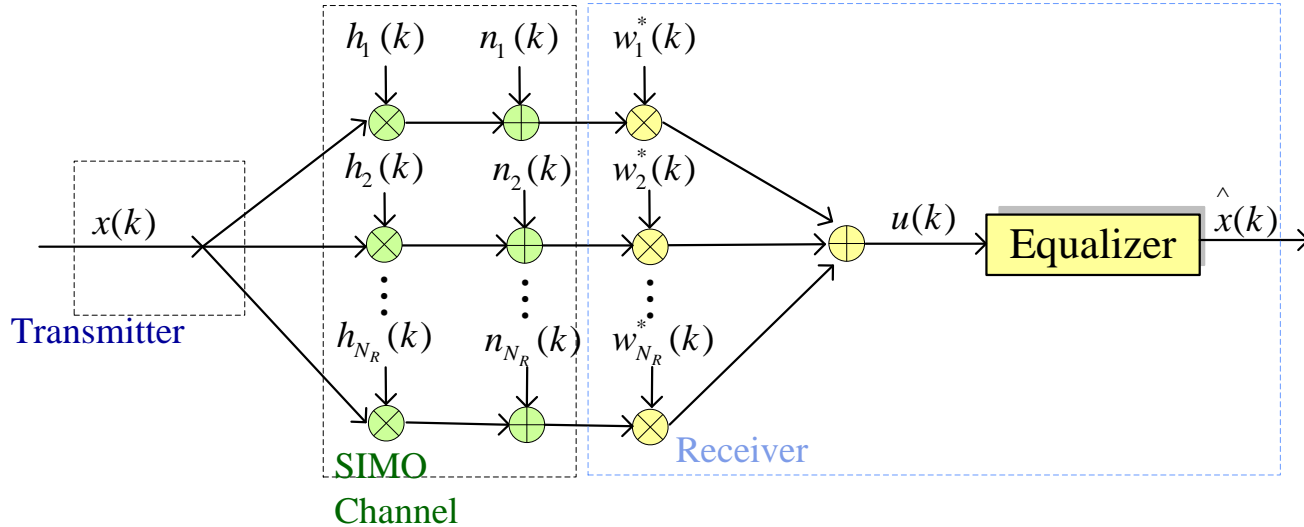
$$\hat{x} = \frac{y}{\alpha} = x + \frac{n}{\alpha}$$

$$\mathbf{p} = \frac{\mathbf{h}^*}{\|\mathbf{h}\|}$$

The post-processing SNR

$$\gamma = \frac{E_s}{N_0} \|\mathbf{h}\|^2$$

Receive MRC



Signal model

$$u = \sum_{i=1}^{N_R} w_i^* h_i x + w_i^* n_i = \mathbf{w}^H \mathbf{h} x + \mathbf{w}^H \mathbf{n}$$

$$\beta$$

$$\hat{x} = \frac{u}{\beta} = x + \frac{\mathbf{w}^H \mathbf{n}}{\beta}$$

The post-processing SNR

$$\mathbf{w} = \mathbf{h}$$

$$\gamma = \frac{E_s}{N_0} \|\mathbf{h}\|^2$$

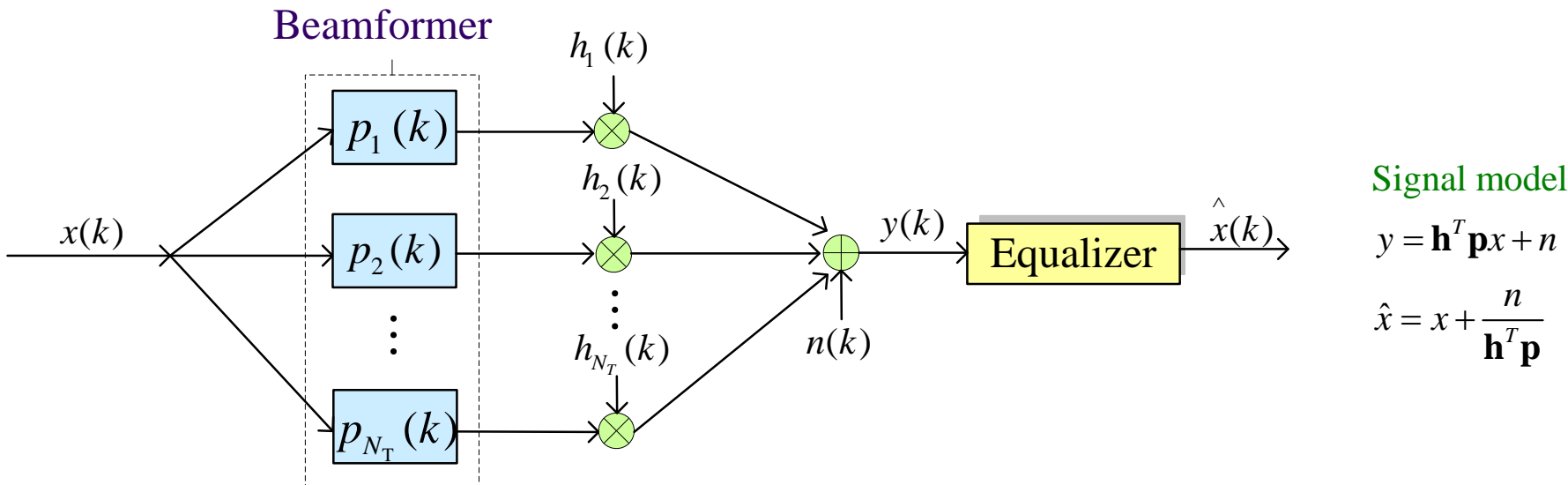


CCU Comm
Smart Antenna Lab

Optimal Beamformer



Based on the Various Performance Metrics



The Performance Metrics

Post - processing SNR $\gamma = \frac{E_s}{N_0} |\mathbf{h}^T \mathbf{p}|^2 \Rightarrow \arg \max_{\|\mathbf{p}\|^2=1} \gamma$

Mean squared error $MSE = E\{ |\hat{x} - x|^2 \} \Rightarrow \arg \min_{\|\mathbf{p}\|^2=1} MSE$

Bit error rate $P_b = \alpha_1 Q\left(\sqrt{\alpha_2 \gamma}\right) \Rightarrow \arg \min_{\|\mathbf{p}\|^2=1} P_b$

Channel capacity $C = \log_2 \left[1 + \frac{E_s}{N_0} |\mathbf{h}^T \mathbf{p}|^2 \right] \Rightarrow \arg \max_{\|\mathbf{p}\|^2=1} C$

$$\arg \max_{\mathbf{p}} |\mathbf{h}^T \mathbf{p}|^2$$

s.t. $\|\mathbf{p}\|^2 = 1$

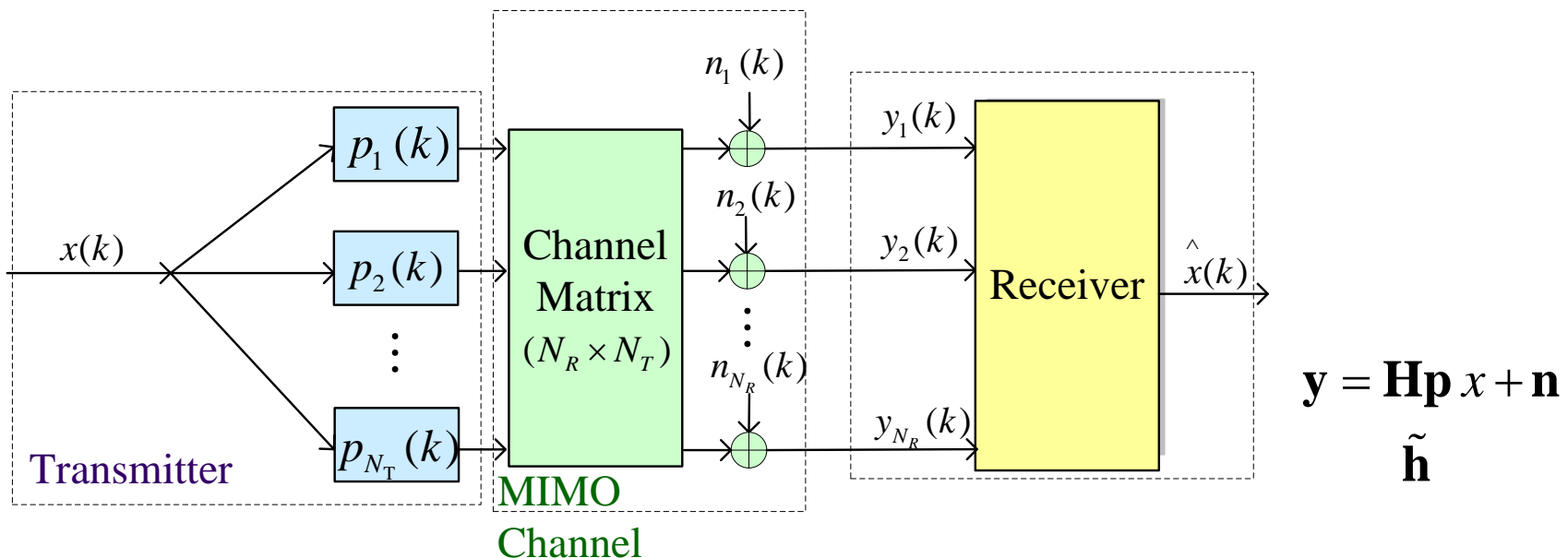
The optimal beamformer

$$\mathbf{p} = \frac{\mathbf{h}^*}{\|\mathbf{h}\|}$$





Transmit Beamforming with Multiple Receive Antennas



Receive MRC

$$\mathbf{w} = \tilde{\mathbf{h}}$$

$$u = \mathbf{w}^H \mathbf{y} = \mathbf{w}^H \tilde{\mathbf{h}} x + \mathbf{w}^H \mathbf{n} = \tilde{\mathbf{h}}^H \tilde{\mathbf{h}} x + \tilde{\mathbf{h}}^H \mathbf{n} \xrightarrow{\text{Equalizer}} \hat{x} = \frac{u}{\|\tilde{\mathbf{h}}\|^2} = x + \frac{\tilde{\mathbf{h}}^H \mathbf{n}}{\|\tilde{\mathbf{h}}\|^2}$$

ZF detection

$$\hat{x} = (\tilde{\mathbf{h}}^H \tilde{\mathbf{h}})^{-1} \tilde{\mathbf{h}}^H \mathbf{y} = \frac{\tilde{\mathbf{h}}^H \mathbf{y}}{\|\tilde{\mathbf{h}}\|^2} = x + \frac{\tilde{\mathbf{h}}^H \mathbf{n}}{\|\tilde{\mathbf{h}}\|^2}$$

The instantaneous SNR at the detection output is $\gamma = \frac{\mathbb{E}\{|x|^2\}}{\mathbb{E}\{|\tilde{\mathbf{h}}^H \mathbf{n}|^2\}} \|\tilde{\mathbf{h}}\|^4 = \frac{E_s}{N_0} \|\tilde{\mathbf{h}}\|^2 = \frac{E_s}{N_0} \|\mathbf{H}\mathbf{p}\|^2$.



Transmit Beamforming with Multiple Receive Antennas

The optimal beamforming vector that maximizes the instantaneous SNR is expressed as

$$\begin{aligned} & \arg \max_{\mathbf{p}} \|\mathbf{H}\mathbf{p}\|^2 \\ \text{s.t. } & \|\mathbf{p}\|^2 = 1 \end{aligned}$$

The solution of the optimal problem turns out to be the right singular vector corresponding to the largest singular value of the channel matrix.

$$N = \min\{N_T, N_R\}$$

$$\mathbf{H} = \mathbf{U}\Sigma\mathbf{V}^H = [\mathbf{u}_1 \quad \mathbf{u}_2 \quad \cdots \quad \mathbf{u}_N] \begin{bmatrix} \sigma_1 & & & \mathbf{0} \\ & \sigma_2 & & \\ & & \ddots & \\ \mathbf{0} & & & \sigma_N \end{bmatrix} [\mathbf{v}_1 \quad \mathbf{v}_2 \quad \cdots \quad \mathbf{v}_N]^H \quad \text{where} \quad \begin{array}{l} \mathbf{U} \in \mathbb{C}^{N_R \times N} \\ \mathbf{V} \in \mathbb{C}^{N_T \times N} \\ \sigma_1 \geq \sigma_2 \geq \cdots \geq \sigma_N \geq 0 \end{array}$$

Let $\mathbf{p} = \mathbf{v}_1 \Rightarrow \mathbf{y} = \mathbf{H}\mathbf{v}_1 x + \mathbf{n} = \sigma_1 \mathbf{u}_1 x + \mathbf{n}$

$$\mathbf{H}\mathbf{v}_1 = \mathbf{U}\Sigma\mathbf{V}^H\mathbf{v}_1 = \mathbf{U}\Sigma \begin{bmatrix} \mathbf{v}_1^H \mathbf{v}_1 \\ \mathbf{v}_2^H \mathbf{v}_1 \\ \vdots \end{bmatrix} = \mathbf{U}\Sigma \begin{bmatrix} 1 \\ 0 \\ \vdots \end{bmatrix} = \mathbf{U} \begin{bmatrix} \sigma_1 \\ 0 \\ \vdots \end{bmatrix} = \sigma_1 \mathbf{u}_1$$

The instantaneous SNR

$$\gamma = \frac{E_s}{N_0} \|\sigma_1 \mathbf{u}_1\|^2 = \frac{E_s}{N_0} \sigma_1^2$$





Based on the Various Performance Metrics

Signal model $\mathbf{y} = \mathbf{H}\mathbf{p}x + \mathbf{n}$

ZF detection $\hat{x} = x + \frac{(\mathbf{H}\mathbf{p})^H \mathbf{n}}{\|\mathbf{H}\mathbf{p}\|^2}$

The Performance Metrics

Post-processing SNR $\gamma = \frac{E_s}{N_0} \|\mathbf{H}\mathbf{p}\|^2 \Rightarrow \arg \max_{\|\mathbf{p}\|^2=1} \gamma$

Mean squared error $MSE = E\{ |\hat{x} - x|^2 \} \Rightarrow \arg \min_{\|\mathbf{p}\|^2=1} MSE$

Bit error rate $P_b = \alpha_1 Q\left(\sqrt{\alpha_2 \gamma}\right) \Rightarrow \arg \min_{\|\mathbf{p}\|^2=1} P_b$



Channel capacity $C = \log_2 \det \left[\mathbf{I} + \frac{E_s}{N_0} (\mathbf{H}\mathbf{p})(\mathbf{H}\mathbf{p})^H \right]$

$$\begin{aligned} & \arg \max_{\mathbf{p}} \mathbf{h}^T \mathbf{p}^2 \\ \text{s.t. } & \|\mathbf{p}\|^2 = 1 \end{aligned}$$

The optimal beamformer

$$\mathbf{p} = \mathbf{v}_1$$

$$= \log_2 \left[1 + \frac{E_s}{N_0} \sigma_1^2 \right] \Rightarrow \arg \max_{\|\mathbf{p}\|^2=1} C$$

singular value of $\mathbf{H}\mathbf{p}$

$$\Rightarrow \|\mathbf{H}\mathbf{p}\|^2$$

$$\begin{aligned} C &= \log_2 \det \left[\mathbf{I} + \rho \mathbf{A} \mathbf{A}^H \right] \\ &= \sum_{i=1}^K \log_2 \left[1 + \rho \sigma_i^2 \right] \end{aligned}$$





Transmit Beamforming with One Spatial Stream

	Signal model	Estimator	The optimal beamformer	The Post-processing SNR
One receive antenna	$y = \mathbf{h}^T \mathbf{p}x + n$	$\hat{x} = x + \frac{n}{\mathbf{h}^T \mathbf{p}}$	$\mathbf{p} = \frac{\mathbf{h}^*}{\ \mathbf{h}\ }$	$\gamma = \frac{E_s}{N_0} \ \mathbf{h}\ ^2$
Multiple receive antennas	$\mathbf{y} = \mathbf{H}\mathbf{p}x + \mathbf{n}$	$\hat{x} = x + \frac{(\mathbf{H}\mathbf{p})^H \mathbf{n}}{\ \mathbf{H}\mathbf{p}\ ^2}$	$\mathbf{p} = \mathbf{v}_1$	$\gamma = \frac{E_s}{N_0} \sigma_1^2$

